12 COMMON PLASTICITY MODELS

Having in Chapter 10 derived the general format of plasticity, it is of interest to consider some specific models. We will discuss various typical plasticity models, evaluate their range of applicability and establish the tangential stiffness matrix $\boldsymbol{D}^{ep}$ that is of importance in nonlinear finite element calculations.

The exposition will mainly be based on the von Mises yield criterion, since it is the standard criterion used for metals and steel. Isotropic, kinematic and mixed hardening of a von Mises material will be discussed and their benefits and shortcomings will be illustrated, and, as an example of a plasticity model for anisotropic materials, a formulation based on Hill's criterion will be presented. Finally, isotropic hardening of a nonassociated Drucker-Prager material will be treated and taken as a simplistic prototype for frictional materials like concrete, soil and rocks.

In the present chapter we will also illustrate the difficulties in modeling of nonlinear kinematic hardening and therefore only linear kinematic hardening will be treated. The next chapter is then entirely devoted to various fairly recent approaches to capturing nonlinear kinematic hardening.

Evidently, a number of other and more advanced plasticity models exist, but from a conceptual point of view most of these models are generalizations of the models treated here and in the next chapter. With the background presented here, the reader should have sufficient information to be able to consult and evaluate the more specialized literature, whenever necessary. We may also mention that several aspects of the specific plasticity models discussed in this chapter may be used when formulating viscoplastic and creep models, cf. Chapter 15.

The present chapter deals only with smooth yield surfaces; the treatment of non-smooth yield criteria that includes, for instance, the Tresca and the Coulomb criteria will be postponed until Chapter 22.

A number of algebraic manipulations are often encountered when a specific plasticity model is considered and in order not to lose the perspective, it is appropriate to recall that all models fit into the general framework discussed in Chapter 10. In particular, the fundamental equations treated in Section 10.1 are here of importance.

Before some typical plasticity models are presented, we will discuss some general experimental characteristics for the plastic response of different groups of materials.

12.1 Experimental characteristics

As previously mentioned, the general experimental evidence for metals and steel shows that the volumetric response is linear elastic and that all nonlinearity is related to the deviatoric response. It turns out that it suffices to adopt associated plasticity theory for these materials. Since the volumetric response is linear, we have plastic incompressibility and referring to (9.85), this implies that the yield criterion does not depend on the first stress invariant $I_1 = \sigma_{kk}$.

For concrete, soil and rocks, the volumetric and deviatoric responses are coupled and both the volumetric and deviatoric responses are nonlinear. To obtain accurate predictions, it is often necessary to adopt nonassociated plasticity theory. Since the response is greatly influenced by the hydrostatic stress, the invariant $I_1 = \sigma_{kk}$ must be included in the formulation and this leads to plastic *compressibility* as well as plastic *dilatancy* depending on the particular load situation, cf. Fig. 4.10b).

Some further experimental characteristics will now be discussed. As cyclic response of metals and steel is often of importance in applications, we will first provide a qualitative discussion of some aspects related to this behavior. For more detail, the reader is referred to Chaboche (1989); Chaboche (1989), Drucker and Palgen (1981), Khan and Huang (1995), Krempl (1971), Lemaitre and Chaboche (1990) and Morrow (1965).

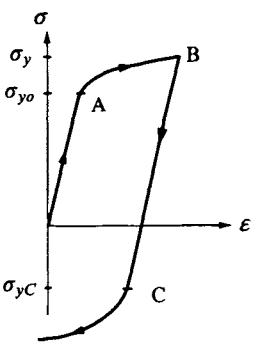

Figure 12.1: Bauschinger effect.

In Chapter 9, we discussed the Bauschinger effect, cf. Fig. 12.1. On reversing the loading from point B, plasticity is again invoked already at point C. The

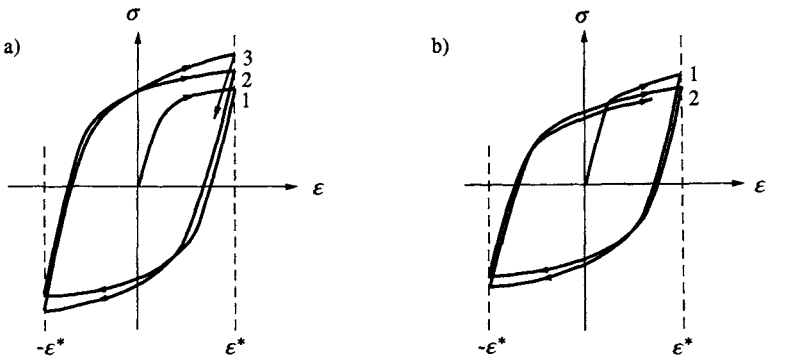

Figure 12.2: Strain cycling between ε^* and $-\varepsilon^*$; a) cyclic hardening; b) cyclic softening.

Bauschinger effect is the observation that the yield stress σ_{yc} at point C is much less than the yield stress σ_y at point B, i.e. $\sigma_{yc} < \sigma_y$.

Often, cycling between different load levels is encountered. If the material is cycled between fixed total strain values, we have *strain cycling*. In the case where the total strain cycles symmetrically between the fixed values ε^* and $-\varepsilon^*$, the situation shown in Fig. 12.2 arises. In Fig. 12.2a), the stress amplitude first increases in each cycle and this phenomenon is called *cyclic hardening*. Eventually, after several cycles, the stress-strain curve repeats itself in each cycle and we have then reached the so-called *stabilized cyclic stress-strain curve*. In Fig. 12.2b), the stress amplitude first decreases in each cycle, i.e. we have *cyclic softening* and, eventually, the stabilized cyclic stress-strain curve is obtained. Whether we have cyclic hardening or softening depends on the particular material in question. Often, a high strength steel is cyclic softening whereas a mild steel is cyclic hardening.

If the material is cycled between fixed stress values, we have *stress cycling*. In the case where the stress cycles symmetrically between the fixed values σ^* and $-\sigma^*$, the situation shown in Fig. 12.3 may be obtained. Cyclic hardening now manifests itself in the form given in Fig. 12.3a) whereas cyclic softening is shown in Fig. 12.3b).

For cycling between fixed strain values that are not symmetrically located about zero, we have, in general, the situation shown in Fig. 12.4. The mean stress is defined as the mean of the maximum and minimum stress in each cycle. It appears that the mean stress decreases with the number of cycles and one speaks of *mean stress relaxation.*

Finally, for cycling between fixed stress values that are not symmetrically located about zero, the situation shown in Fig. 12.5 arises. After each cycle, the total strain increases and one speaks of a *ratcheting effect.* Moreover, the ratcheting occurs in the 'direction' of the mean stress. Referring to Fig. 12.5, the

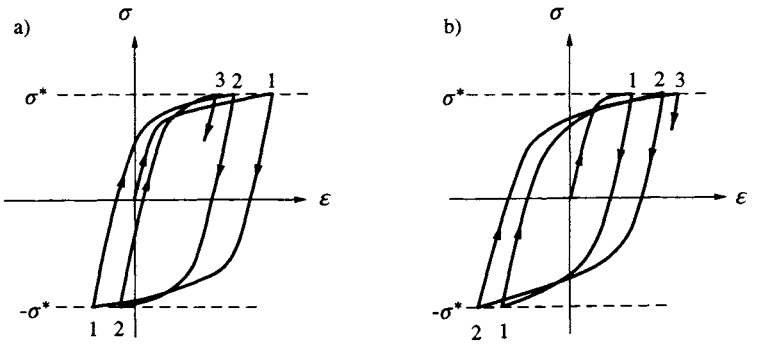

Figure 12.3: Stress cycling between σ^* and $-\sigma^*$; a) cyclic hardening; b) cyclic softening.

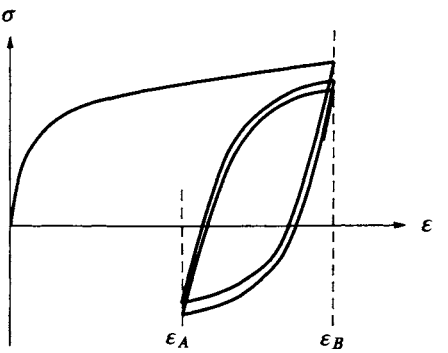

Figure 12.4: Strain cycling between the unsymmetric strain values ε_A and ε_B; mean stress relaxation.

mean stress is positive, i.e. the ratcheting results in an increasing strain. Instead of speaking of a ratcheting effect, the terminology of cyclic creep is often used in the literature, but this terminology seems not to be entirely appropriate since no creep effects – i.e. time-dependent material properities – are present.

For concrete, soil or rocks the influence of the hydrostatic stress as well as the coupling between volumetric and deviatoric response complicate the response and thereby the requirements on an accurate constitutive model. Plasticity models are therefore mostly used for load situations where significant cycling does not occur and we may therefore restrict ourselves to the illustration given in Fig. 12.6. Concrete is here loaded triaxially along the compressive meridian, cf. (8.22); first a purely hydrostatic loading is applied and then $\sigma_1 = \sigma_2$ is kept constant while σ_3 is decreased (tension is considered as a positive quantity). The effect of the hydrostatic stress is clearly observed.

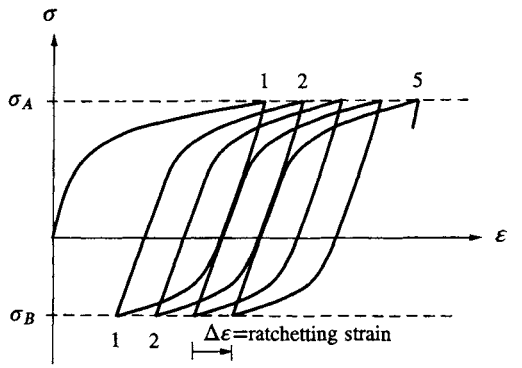

Figure 12.5: Stress cycling between the unsymmetric stress values σ_A and σ_B; ratcheting in the direction of the mean stress.

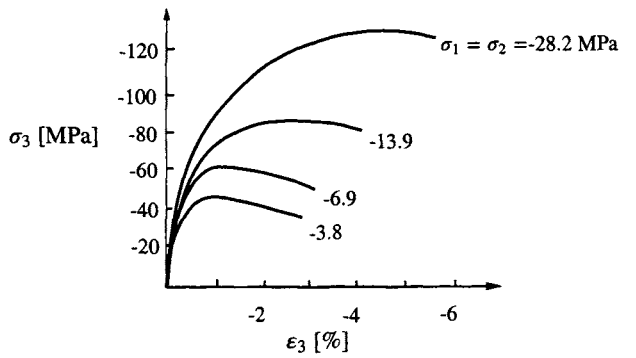

Figure 12.6: Triaxial compression of concrete along the compressive meridian, Richart *et al.* (1928); effect of hydrostatic stress.

It was mentioned above that frictional materials like concrete, soil and rocks may exhibit plastic compressibility as well as plastic dilatancy, i.e. a plastic volume change occurs. This issue complicates the modeling efforts significantly and we will now discuss various aspects of this issue.

For isotropic materials, where the potential function g may be written in the form $g = g(I_1, J_2, J_3, K_\alpha)$, (9.83) and (9.85) lead to

$$\dot{\varepsilon}_{ii}^p = \dot{\lambda} 3 \frac{\partial g}{\partial I_1}$$

i.e., frictional materials require that the first stress invariant I_1 is included in the formulation. The relation between the plastic volume change and the form of the potential surface may perhaps be more easily seen by the following arguments.

Considering isotropic materials, a general expression for $\partial g / \partial \sigma_{ij}$ is given by (9.84). If the coordinate system is chosen collinear with the principal directions

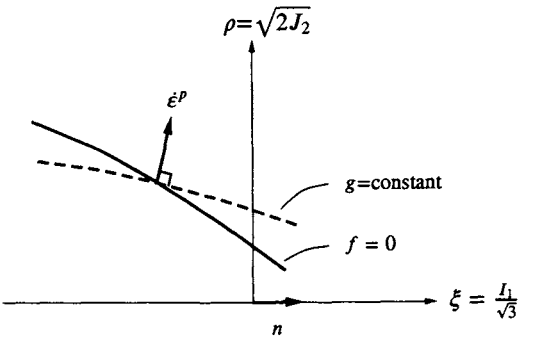

Figure 12.7: Meridian plane and illustration of $\dot{\varepsilon}^p$ being normal to the potential surface. In the present case, a plastic volume increase will occur.

of the stress tensor then σ_{ij} becomes a diagonal matrix; consequently, both s_{ij} as well as $s_{ik}s_{kj}$ become diagonal matrices. In turn, this implies that also $\partial g/\partial\sigma_{ij}$ becomes diagonal, i.e. $\dot{\varepsilon}^p_{ij}$ and σ_{ij} possess the same principal directions.

We now adopt the Haigh-Westergaard coordinate system where the principal stresses σ_1, σ_2 and σ_3 are measured along the axes, cf. Fig. 8.4. Since the principal directions for σ_{ij} and $\dot{\varepsilon}^p_{ij}$ coincide, we can also measure the principal plastic strain rates $\dot{\varepsilon}^p_1$, $\dot{\varepsilon}^p_2$ and $\dot{\varepsilon}^p_3$ along these axes. Introduce for the moment the notation

$$\dot{\boldsymbol{\varepsilon}}^p = \begin{bmatrix} \dot{\varepsilon}^p_1 \\ \dot{\varepsilon}^p_2 \\ \dot{\varepsilon}^p_3 \end{bmatrix} \tag{12.1}$$

The potential surface g = constant describes a surface in the Haigh-Westergaard coordinate system. According to the flow rule, the plastic strain rate $\dot{\varepsilon}^p_{ij}$ is normal to the potential surface. That is, in the Haigh-Westergaard coordinate system, the vector $\dot{\boldsymbol{\varepsilon}}^p$ defined by (12.1) is normal to the potential surface. The vector $\dot{\boldsymbol{\varepsilon}}^p$ is therefore also normal to the meridians of the potential surface as illustrated in Fig. 12.7.

Define the unit vector $\boldsymbol{n}$ in the Haigh-Westergaard coordinate system according to

$$\boldsymbol{n} = \frac{1}{\sqrt{3}} \begin{bmatrix} 1 \\ 1 \\ 1 \end{bmatrix} \tag{12.2}$$

In accordance with Fig. 8.4, this unit vector is located along the hydrostatic axis, i.e. it takes the direction shown in Fig. 12.7. We have

$$\dot{\varepsilon}^p_{ii} = \dot{\varepsilon}^p_{11} + \dot{\varepsilon}^p_{22} + \dot{\varepsilon}^p_{33} = \dot{\varepsilon}^p_1 + \dot{\varepsilon}^p_2 + \dot{\varepsilon}^p_3$$

which with (12.1) and (12.2) may be written as

$$\dot{\varepsilon}_{ii}^p = \sqrt{3}\boldsymbol{n}^T\dot{\boldsymbol{\varepsilon}}^p \tag{12.3}$$

As an illustration of the use of this expression, we have plastic dilatancy if the meridians of the potential surface open in the direction of the negative hydrostatic axis; this situation is illustrated in Fig. 12.7.

For metals and steel, we have plastic incompressibility $\dot{\varepsilon}_{ii}^p = 0$, i.e. the plastic strain rate $\dot{\varepsilon}_{ij}^p$ is purely deviatoric. For frictional materials, however, the plastic strain rate $\dot{\varepsilon}_{ij}^p$ also involves a volumetric component. The flow rule states that $\dot{\varepsilon}_{ij}^p = \dot{\lambda}\partial g/\partial\sigma_{ij}$ and since $\dot{\varepsilon}_{ij}^p$ for frictional materials is more complex than $\dot{\varepsilon}_{ij}^p$ for metals and steel, the requirements to the potential function g are also more complex. It is therefore to be expected that whereas for metals and steel it suffices to adopt an associated flow rule, frictional materials require, in general, a nonassociated flow rule. This expectation is supported by modeling experience.

12.2 Isotropic von Mises hardening

This model is based on associated plasticity and it is of relevance for the response of metals and steel for which significant reversed loadings do not occur. The model was treated to some extent in Section 9.6 and we will here provide the general format of this model that is applicable in nonlinear finite element schemes as well as a discussion of its prediction capabilities. For evident reasons, von Mises plasticity theory is often called *J_2-plasticity*.

Recognizing (9.20), the yield criterion is given by

$$\boxed{f(\sigma_{ij}, K) = (\frac{3}{2}s_{kl}s_{kl})^{1/2} - \sigma_y \;;\quad f = 0 \;;\quad \sigma_y = \sigma_{yo} + K(\kappa)} \tag{12.4}$$

i.e.

$$\frac{\partial f}{\partial\sigma_{ij}} = \frac{3}{2}\frac{s_{ij}}{\sigma_y}\;;\qquad \frac{\partial f}{\partial K} = -1\;;\qquad \frac{\partial K}{\partial\kappa} = \frac{d\sigma_y}{d\kappa} \tag{12.5}$$

The flow rule states that $\dot{\varepsilon}_{ij}^p = \dot{\lambda}\partial f/\partial\sigma_{ij}$, i.e.

$$\dot{\varepsilon}_{ij}^p = \dot{\lambda}\frac{3s_{ij}}{2\sigma_y} \tag{12.6}$$

It follows that we have plastic incompressibility, i.e $\dot{\varepsilon}_{kk}^p = 0$. The evolution law (10.13) for the internal variable κ is

$$\dot{\kappa} = \dot{\lambda}k(\sigma_{ij}, K) \tag{12.7}$$

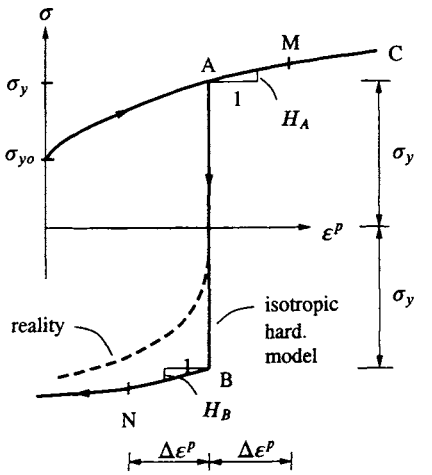

Figure 12.8: Uniaxial loading. Effects of reversed loading; $H_B = H_A$ and $H_N = H_M$.

The consistency relation $\dot{f} = 0$ yields

$$\frac{\partial f}{\partial \sigma_{ij}} \dot{\sigma}_{ij} - H\dot{\lambda} = 0$$

where the plastic modulus H according to (10.17) is defined by

$$H = -\frac{\partial f}{\partial K}\frac{\partial K}{\partial \kappa}k = \frac{d\sigma_y}{d\kappa}k \tag{12.8}$$

Introduce the definitions

$$\boxed{\sigma_{eff} = (\frac{3}{2}s_{kl}s_{kl})^{1/2}\,; \qquad \dot{\varepsilon}^p_{eff} = (\frac{2}{3}\dot{\varepsilon}^p_{ij}\dot{\varepsilon}^p_{ij})^{1/2}} \tag{12.9}$$

i.e. the yield criterion takes the form

$$\sigma_{eff} - \sigma_y(\kappa) = 0$$

and we obtain

$$\dot{\varepsilon}^p_{eff} = \dot{\lambda} \tag{12.10}$$

We choose the strain hardening assumption

$$\dot{\kappa} = \dot{\varepsilon}^p_{eff} \quad \text{i.e.} \quad \dot{\kappa} = \dot{\lambda} \tag{12.11}$$

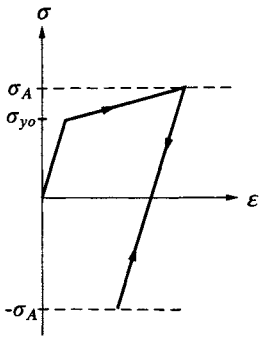

Figure 12.9: Effects of stress cycling between σ_A and $-\sigma_A$; elastic shake-down.

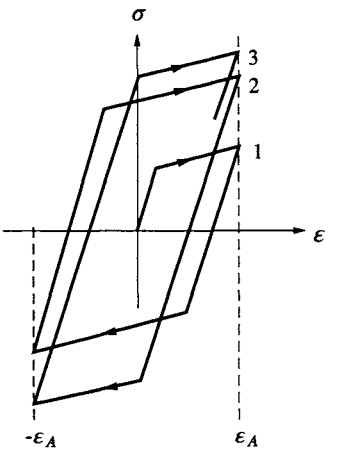

Figure 12.10: Effects of strain cycling between ε_A and $-\varepsilon_A$.

This means that $\sigma_y = \sigma_y(\kappa)$ becomes $\sigma_y = \sigma_y(\varepsilon^p_{eff})$. A comparison of (12.11b) with (12.7) shows that $k = 1$ and (12.8) then leads to the following expression for the plastic modulus

$$\boxed{H = \frac{d\sigma_y(\varepsilon^p_{eff})}{d\varepsilon^p_{eff}}} \tag{12.12}$$

Moreover, $K = K(\kappa)$ and (12.11) implies

$$\dot{K} = \frac{dK}{d\kappa}\dot{\lambda} \tag{12.13}$$

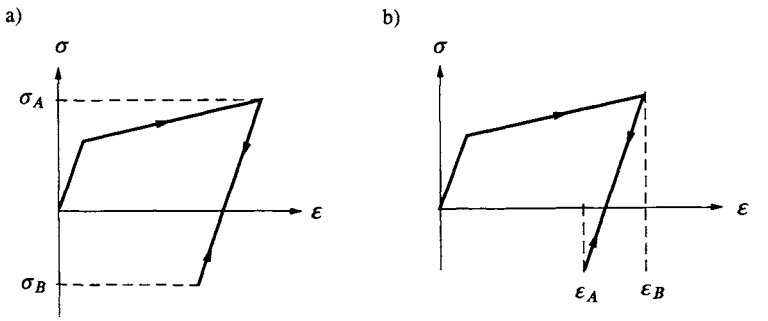

Figure 12.11: a) unsymmetric stress cycling, no ratcheting; b) unsymmetric strain cycling, no mean stress relaxation.

For uniaxial loading (tension or compression), we have $|\sigma| = \sigma_{eff} = \sigma_y$ and $|d\varepsilon^p| = d\varepsilon^p_{eff}$ and the implications of (12.12) are illustrated in Fig. 12.8. If we reverse the loading at point A, plasticity is again activated at point B where $\sigma_B = -\sigma_A$. Referring to Fig. 12.1, we conclude that the Bauschinger effect is not modeled. According to (12.12), the slope at point A is H_A and since no change occurs in the internal variable ε^p_{eff} during the elastic response from point A to B, we have the same slope at point B, i.e. $H_B = H_A$. As $\dot{\varepsilon}^p_{eff} \geq 0$, the effective plastic strain always accumulates the plastic strain contributions and for uniaxial loading, we have $\dot{\varepsilon}^p_{eff} = |\dot{\varepsilon}^p|$. Therefore, the effective plastic strains at points M and N are identical and it follows that the slopes at points M and N are the same. The real response during reversed loading is also indicated in Fig. 12.8, and it appears that the isotropic hardening model provides a rather inferior prediction.

For the purpose of evaluating cyclic loading, we adopt for simplicity linear hardening, i.e. H becomes a constant. If the loading cycles between the stress states $\pm\sigma_A$, we obtain the result illustrated in Fig. 12.9; as the response is purely elastic during cycling, one speaks of an immediate *elastic shake-down*. If the loading cycles between the strain states $\pm\varepsilon_A$, isotropic hardening predicts the cyclic hardening behavior shown in Fig. 12.10. After an infinitely large number of strain cycles, the isotropic hardening model will predict a cyclic behavior that is purely elastic.

For cycling between unsymmetric stress states, the isotropic hardening model predicts the response shown in Fig. 12.11a); no ratcheting is predicted and elastic shake-down occurs immediately. Figure 12.11b) shows cycling between unsymmetric strain states and it appears that no mean stress relaxation is predicted.

The discussion relating to Figs. 12.8-12.11 clearly emphasizes that isotropic hardening is applicable when continued plastic loading is involved whereas the effect of significant reversed loadings cannot be modeled in a proper fashion.

In order to determine the tangential elasto-plastic stiffness matrix $\boldsymbol{D}^{ep}$ of

relevance in nonlinear finite element calculations, we shall assume isotropic elasticity, i.e. (4.89) provides

$$D_{ijkl} = 2G\left[\frac{1}{2}(\delta_{ik}\delta_{jl} + \delta_{il}\delta_{jk}) + \frac{\nu}{1-2\nu}\delta_{ij}\delta_{kl}\right] \tag{12.14}$$

We then obtain with (12.5)

$$\frac{\partial f}{\partial \sigma_{mn}} D_{mnkl} = 3G\frac{s_{kl}}{\sigma_y}; \qquad D_{ijst}\frac{\partial f}{\partial \sigma_{st}} = 3G\frac{s_{ij}}{\sigma_y}$$

and (10.24) then yields

$$A = H + 3G$$

With these expressions, (10.26) and (10.27) give

$$\dot{\sigma}_{ij} = D^{ep}_{ijkl}\dot{\epsilon}_{kl} \tag{12.15}$$

where

$$D^{ep}_{ijkl} = D_{ijkl} - \frac{9G^2}{A}\frac{s_{ij}s_{kl}}{\sigma_y^2} \tag{12.16}$$

If we express (12.15) in a matrix form similar to (4.37), we arrive at

$$\dot{\boldsymbol{\sigma}} = \boldsymbol{D}^{ep}\dot{\boldsymbol{\epsilon}} \tag{12.17}$$

where

$$\boldsymbol{D}^{ep} = \boldsymbol{D} - \boldsymbol{D}^{p} \tag{12.18}$$

and

$$\boldsymbol{D} = \frac{2G}{1-2\nu}\begin{bmatrix} 1-\nu & \nu & \nu & 0 & 0 & 0 \\ \nu & 1-\nu & \nu & 0 & 0 & 0 \\ \nu & \nu & 1-\nu & 0 & 0 & 0 \\ 0 & 0 & 0 & \frac{1}{2}(1-2\nu) & 0 & 0 \\ 0 & 0 & 0 & 0 & \frac{1}{2}(1-2\nu) & 0 \\ 0 & 0 & 0 & 0 & 0 & \frac{1}{2}(1-2\nu) \end{bmatrix} \tag{12.19}$$

$$\boldsymbol{D}^{p} = \frac{9G^2}{A\sigma_y^2}\begin{bmatrix} s_{11}^2 & s_{11}s_{22} & s_{11}s_{33} & s_{11}s_{12} & s_{11}s_{13} & s_{11}s_{23} \\ s_{22}s_{11} & s_{22}^2 & s_{22}s_{33} & s_{22}s_{12} & s_{22}s_{13} & s_{22}s_{23} \\ s_{33}s_{11} & s_{33}s_{22} & s_{33}^2 & s_{33}s_{12} & s_{33}s_{13} & s_{33}s_{23} \\ s_{12}s_{11} & s_{12}s_{22} & s_{12}s_{33} & s_{12}^2 & s_{12}s_{13} & s_{12}s_{23} \\ s_{13}s_{11} & s_{13}s_{22} & s_{13}s_{33} & s_{13}s_{12} & s_{13}^2 & s_{13}s_{23} \\ s_{23}s_{11} & s_{23}s_{22} & s_{23}s_{33} & s_{23}s_{12} & s_{23}s_{13} & s_{23}^2 \end{bmatrix} \tag{12.20}$$

The $\boldsymbol{D}^{ep}$-matrix is clearly symmetric. It is of interest that even though isotropic elasticity is adopted, we have a fully populated $\boldsymbol{D}^{ep}$-matrix, i.e. we have coupling effects between normal stresses and shear strains as well as between shear stresses and normal strains. Moreover, by setting $H = 0$ and $\sigma_y = \sigma_{yo}$, which implies that $A = 3G$, the formulation above also holds for ideal plasticity.

12.2.1 Plane strain

For plane strain, i.e. $\dot{\varepsilon}_{13} = \dot{\varepsilon}_{23} = \dot{\varepsilon}_{33} = 0$, (12.17)-(12.20) directly provide

$$\dot{\boldsymbol{\sigma}} = \boldsymbol{D}^{ep}\dot{\boldsymbol{\varepsilon}} \tag{12.21}$$

where

$$\boldsymbol{D}^{ep} = \boldsymbol{D} - \boldsymbol{D}^{p} \tag{12.22}$$

and

$$\boldsymbol{D} = \frac{2G}{1-2\nu}\begin{bmatrix} 1-\nu & \nu & 0 \\ \nu & 1-\nu & 0 \\ 0 & 0 & \frac{1}{2}(1-2\nu) \end{bmatrix} \tag{12.23}$$

$$\boldsymbol{D}^{p} = \frac{9G^2}{A\sigma_y^2}\begin{bmatrix} s_{11}^2 & s_{11}s_{22} & s_{11}s_{12} \\ s_{22}s_{11} & s_{22}^2 & s_{22}s_{12} \\ s_{12}s_{11} & s_{12}s_{22} & s_{12}^2 \end{bmatrix} \tag{12.24}$$

Moreover, considering the out-of-plane stresses, we obtain from (12.17)-(12.20)

$$\begin{bmatrix} \dot{\sigma}_{33} \\ \dot{\sigma}_{13} \\ \dot{\sigma}_{23} \end{bmatrix} = \frac{2G}{1-2\nu}\begin{bmatrix} \nu & \nu & 0 \\ 0 & 0 & 0 \\ 0 & 0 & 0 \end{bmatrix}\begin{bmatrix} \dot{\varepsilon}_{11} \\ \dot{\varepsilon}_{22} \\ 2\dot{\varepsilon}_{12} \end{bmatrix} - \frac{9G^2}{A\sigma_y^2}\begin{bmatrix} s_{33}s_{11} & s_{33}s_{22} & s_{33}s_{12} \\ s_{13}s_{11} & s_{13}s_{22} & s_{13}s_{12} \\ s_{23}s_{11} & s_{23}s_{22} & s_{23}s_{12} \end{bmatrix}\begin{bmatrix} \dot{\varepsilon}_{11} \\ \dot{\varepsilon}_{22} \\ 2\dot{\varepsilon}_{12} \end{bmatrix}$$

It appears that $\sigma_{13} = s_{13} = 0$ and $\sigma_{23} = s_{23} = 0$ hold in the elastic region before any plasticity occurs. The expression above therefore implies that $\dot{\sigma}_{13} = \dot{\sigma}_{23} = 0$ holds at the event that plasticity is initiated, i.e. $\sigma_{13} = \sigma_{23} = 0$ holds in general. It is concluded that

$$\sigma_{13} = \sigma_{23} = 0 \tag{12.25}$$

and

$$\dot{\sigma}_{33} = \frac{2G\nu}{1-2\nu}(\dot{\varepsilon}_{11} + \dot{\varepsilon}_{22}) - \frac{9G^2}{A\sigma_y^2}s_{33}(s_{11}\dot{\varepsilon}_{11} + s_{22}\dot{\varepsilon}_{22} + 2s_{12}\dot{\varepsilon}_{12})$$

To determine the out-of-plane plastic strain components, we obtain from (12.6)

$$\dot{\varepsilon}_{i3}^{p} = \dot{\lambda}\frac{3s_{i3}}{2\sigma_y}$$

From (12.25), we conclude

$$\varepsilon_{13}^{p} = \varepsilon_{23}^{p} = 0\,; \quad \dot{\varepsilon}_{33}^{p} = \dot{\lambda}\frac{3s_{33}}{2\sigma_y}$$

where $\dot{\lambda} = \dot{\varepsilon}_{eff}^{p}$.

12.2.2 Plane stress

For plane stress, i.e. $\sigma_{13} = \sigma_{23} = \sigma_{33} = 0$, the formulation becomes somewhat more involved as already discussed in Section 10.6. From (10.47) and (12.5) follow that

$$D^*_{\alpha\beta\gamma\delta}\frac{\partial f}{\partial \sigma_{\gamma\delta}} = \frac{3G}{\sigma_y}(s_{\alpha\beta} + \frac{\nu}{1-\nu}\delta_{\alpha\beta}s_{\gamma\gamma}) \tag{12.26}$$

i.e., the quantity A^* given by (10.52) becomes

$$A^* = H + \frac{9G}{2\sigma_y^2}(s_{\alpha\beta}s_{\alpha\beta} + \frac{\nu}{1-\nu}s_{\gamma\gamma}s_{\beta\beta}) \tag{12.27}$$

Note, that A^* varies with the loading also for linear hardening, i.e. H=constant. This is in contrast to the general three-dimensional situation and the plane strain case, where H=constant implies that A=constant. From (12.26), we obtain

$$D^*_{\alpha\beta\pi\theta}\frac{\partial f}{\partial \sigma_{\pi\theta}}\frac{\partial f}{\partial \sigma_{\phi\psi}}D^*_{\phi\psi\gamma\delta} = \frac{9G^2}{\sigma_y^2}(s_{\alpha\beta} + \frac{\nu}{1-\nu}\delta_{\alpha\beta}s_{\theta\theta})(s_{\gamma\delta} + \frac{\nu}{1-\nu}\delta_{\gamma\delta}s_{\pi\pi})$$

With (10.54) and (4.112) it then follows that

$$\dot{\boldsymbol{\sigma}} = \boldsymbol{D}^{*ep}\dot{\boldsymbol{\varepsilon}} \tag{12.28}$$

where

$$\boldsymbol{D}^{*ep} = \boldsymbol{D}^* - \boldsymbol{D}^{*p} \tag{12.29}$$

and

$$\boldsymbol{D}^* = \frac{E}{1-\nu^2}\begin{bmatrix} 1 & \nu & 0 \\ \nu & 1 & 0 \\ 0 & 0 & \frac{1}{2}(1-\nu) \end{bmatrix} \tag{12.30}$$

$$\boldsymbol{D}^{*p} = \frac{9G^2}{A^*\sigma_y^2(1-\nu)^2}\begin{bmatrix} (s^*_{11})^2 & s^*_{11}s^*_{22} & (1-\nu)s^*_{11}s_{12} \\ s^*_{22}s^*_{11} & (s^*_{22})^2 & (1-\nu)s^*_{22}s_{12} \\ (1-\nu)s_{12}s^*_{11} & (1-\nu)s_{12}s^*_{22} & (1-\nu)^2s^2_{12} \end{bmatrix} \tag{12.31}$$

where

$$s^*_{11} = s_{11} + \nu s_{22}\,; \quad s^*_{22} = s_{22} + \nu s_{11}$$

Finally, for the out-of-plane plastic strain components, (12.6) together with $\sigma_{13} = \sigma_{23} = 0$ yield

$$\varepsilon^p_{13} = \varepsilon^p_{23} = 0\,; \quad \dot{\varepsilon}^p_{33} = \dot{\lambda}\frac{3s_{33}}{2\sigma_y}$$

The plane stress condition implies $s_{33} = -(\sigma_{11} + \sigma_{22})/3$ and, in general, we therefore have $\dot{\varepsilon}^p_{33} \neq 0$. Moreover, it is recalled that $\dot{\lambda} = \dot{\varepsilon}^p_{eff}$

As previously discussed, it is worthwhile to observe that the elasto-plastic relations for plane stress are more involved than those pertinent for the general three-dimensional situation as well as for the plane strain case.

12.3 Kinematic von Mises hardening

Kinematic hardening of a von Mises material is of relevance for metals and steel where reversed loadings are of significance. First, the general properties of kinematic hardening shall be scrutinized. Referring to (9.24), kinematic hardening is, in general, described by

$$f(\sigma_{ij}, K_\alpha) = F(\sigma_{ij} - \alpha_{ij}) = 0 \tag{12.32}$$

where we have one hardening parameter given in terms of the *back-stress tensor* α_{ij}, which describes the center position of the current yield surface.

Considering the initial yield criterion $F(\sigma_{ij}) = 0$, we observed in Chapter 8 that this criterion for an isotropic material may be described, for instance, in terms of

$$F(I_1, J_2, \cos 3\theta) = 0 \tag{12.33}$$

where the stress invariants are defined by

$$I_1 = \sigma_{ii}\,; \quad J_2 = \frac{1}{2}s_{ij}s_{ij}\,; \quad \cos 3\theta = \frac{3\sqrt{3}J_3}{2J_2^{3/2}}$$

and $J_3 = s_{ij}s_{jk}s_{ki}/3$. For metals and steel, the hydrostatic stress I_1 has no influence on yielding, i.e. (12.33) reduces to $F(J_2, \cos 3\theta) = 0$. The invariant J_2 provides information of the magnitude of the deviatoric stresses whereas the invariant $\cos 3\theta$ gives information of the direction of the deviatoric stresses. The von Mises criterion was obtained by dropping the influence of the term $\cos 3\theta$, i.e $F(J_2) = 0$ or $\sqrt{3J_2} - \sigma_{yo} = 0$, where σ_{yo} is the initial yield stress in tension.

Let us now treat (12.32) in the same manner. Define the *reduced stress tensor* $\bar{\sigma}_{ij}$ by

$$\bar{\sigma}_{ij} = \sigma_{ij} - \alpha_{ij} \tag{12.34}$$

i.e.

$$\bar{\sigma}_{ii} = \sigma_{ii} - \alpha_{ii}$$

The deviatoric part of the reduced stress tensor is defined by $\bar{s}_{ij} = \bar{\sigma}_{ij} - \delta_{ij}\bar{\sigma}_{kk}/3$ and it becomes

$$\boxed{\bar{s}_{ij} = s_{ij} - \alpha_{ij}^d} \tag{12.35}$$

where α_{ij}^d denotes the deviatoric part of the back-stress tensor α_{ij}, i.e.

$$\alpha_{ij}^d = \alpha_{ij} - \frac{1}{3}\delta_{ij}\alpha_{kk}$$

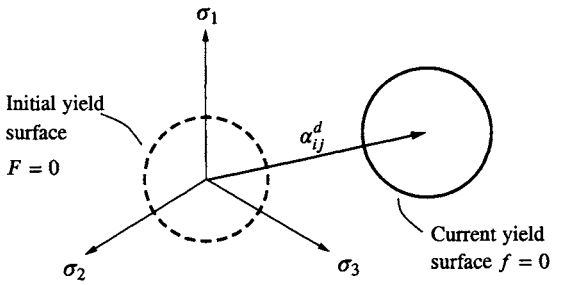

Figure 12.12: Deviatoric plane. Kinematic hardening of a von Mises material.

With (12.34), (12.32) takes the form $F(\tilde{\sigma}_{ij}) = 0$, which, in analogy with (12.33), can be expressed as

$$F(\bar{I}_1, \bar{J}_2, \cos 3\bar{\theta}) = 0 \tag{12.36}$$

where

$$\bar{I}_1 = \bar{\sigma}_{ii}\,; \quad \bar{J}_2 = \frac{1}{2}\bar{s}_{ij}\bar{s}_{ij}\,; \quad \cos 3\bar{\theta} = \frac{3\sqrt{3}\bar{J}_3}{2\bar{J}_2^{3/2}}$$

and $\bar{J}_3 = \bar{s}_{ij}\bar{s}_{jk}\bar{s}_{ki}/3$. Arguing as previously, we ignore the influence of the invariants $\bar{I}_1$ and $\cos 3\bar{\theta}$, i.e. (12.36) reduces to $F(\bar{J}_2) = 0$ or $\sqrt{3\bar{J}_2} - \sigma_{yo} = 0$. With (12.35), we then find for kinematic hardening of a von Mises material that the current yield criterion is given by

$$\boxed{f(\sigma_{ij}, K_\alpha) = \left[\frac{3}{2}(s_{kl} - \alpha_{kl}^d)(s_{kl} - \alpha_{kl}^d)\right]^{1/2} - \sigma_{yo} = 0} \qquad K_\alpha = \{\alpha_{ij}^d\} \tag{12.37}$$

where σ_{yo} is the initial yield stress in tension and it is indicated that the hardening parameters K_α take the form of the back-stress. For $\alpha_{kl}^d = 0$, this expression evidently reduces to the initial von Mises criterion.

The von Mises surface is a cylinder in the stress space and the deviatoric part α_{ij}^d of the back-stress describes the center of this cylinder in the deviatoric plane, as illustrated in Fig. 12.12. Note that in accordance with experimental evidence, cf. Figs. 9.18 and 9.19, the current yield surface does not need to include the origin of the stress space.

After these introductory remarks, the fundamental equations for kinematic hardening of a von Mises material will be presented. From (12.37) it follows that

$$\frac{\partial f}{\partial \sigma_{ij}} = \frac{3(s_{ij} - \alpha_{ij}^d)}{2\sigma_{yo}}\,; \qquad \frac{\partial f}{\partial \alpha_{ij}^d} = -\frac{3(s_{ij} - \alpha_{ij}^d)}{2\sigma_{yo}} \tag{12.38}$$

The flow rule $\dot{\varepsilon}^p_{ij} = \dot{\lambda}\partial f/\partial\sigma_{ij}$ then provides

$$\dot{\varepsilon}^p_{ij} = \dot{\lambda}\,\frac{3(s_{ij} - \alpha^d_{ij})}{2\sigma_{yo}} \tag{12.39}$$

and plastic incompressibility, i.e. $\dot{\varepsilon}^p_{kk} = 0$, follows readily. As usual, the effective plastic strain rate is defined by

$$\dot{\varepsilon}^p_{eff} = (\frac{2}{3}\dot{\varepsilon}^p_{ij}\dot{\varepsilon}^p_{ij})^{1/2}$$

and the flow rule (12.39) as well as the yield criterion (12.37) then imply

$$\dot{\varepsilon}^p_{eff} = \dot{\lambda} \tag{12.40}$$

Let us now evaluate the plastic modulus H. In the present case, we have one hardening parameter in terms of the deviatoric part α^d_{ij} of the back-stress and referring to (10.15) and (10.17), we have

$$\dot{\alpha}^d_{ij} = \dot{\lambda}q_{ij} \quad \text{where} \quad q_{ij} = \frac{\partial\alpha^d_{ij}}{\partial\kappa_{kl}}k_{kl} \tag{12.41}$$

and

$$H = -\frac{\partial f}{\partial\alpha^d_{ij}}q_{ij} \tag{12.42}$$

and where q_{ij} may be considered as a combined evolution function. The consistency relation $\dot{f} = 0$ is written in the standard form as

$$\frac{\partial f}{\partial\sigma_{ij}}\dot{\sigma}_{ij} - H\dot{\lambda} = 0 \tag{12.43}$$

To obtain an interpretation of the plastic modulus H, we multiply the consistency relation (12.43) by $\dot{\lambda}$ and use the flow rule $\dot{\varepsilon}^p_{ij} = \dot{\lambda}\partial f/\partial\sigma_{ij}$ as well as (12.40) to obtain

$$\dot{\varepsilon}^p_{ij}\dot{\sigma}_{ij} - (\dot{\varepsilon}^p_{eff})^2\,H = 0 \tag{12.44}$$

Considering uniaxial stress conditions, the term $\dot{\varepsilon}^p_{ij}\dot{\sigma}_{ij}$ reduces to $\dot{\varepsilon}^p\dot{\sigma}$ and $\dot{\varepsilon}^p_{eff}$ becomes equal to $|\dot{\varepsilon}^p|$. In this case, (12.44) reduces to

$$\boxed{\frac{d\sigma}{d\varepsilon^p} = H} \tag{12.45}$$

This interpretation of H is illustrated in Fig. 12.13.

Let us now choose the specific evolution law to be used, i.e. we have to specify the evolution function q_{ij} present in (12.41). As discussed in relation to (10.17) it is allowable to directly specify the combined evolution function q_{ij}

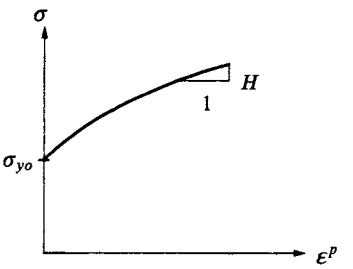

Figure 12.13: Interpretation of plastic modulus H.

instead of specifying the individual factors $\partial\alpha_{ij}^d/\partial\kappa_{kl}$ and k_{kl}. This approach is often advantageous and it is the case when kinematic hardening occurs. The classical kinematic evolution law was proposed by Melan (1938) and later by Prager (1955) and it reads

$$\boxed{\dot{\alpha}_{ij} = c\,\dot{\varepsilon}_{ij}^p \qquad \textit{Melan-Prager's evolution law}} \tag{12.46}$$

where c is a positive material parameter that may depend on the load history. We will later in this chapter discuss other kinematic evolution laws. In the present case of a von Mises material, (12.39) implies $\dot{\varepsilon}_{ii}^p = 0$, i.e. (12.46) shows that $\dot{\alpha}_{ii} = 0$, i.e. the back-stress tensor is a purely deviatoric tensor

$$\alpha_{ij}^d = \alpha_{ij} \tag{12.47}$$

Use of (12.39) into (12.46) then yields

$$\dot{\alpha}_{ij}^d = \dot{\lambda}\frac{3c}{2\sigma_{yo}}(s_{ij} - \alpha_{ij}^d) \tag{12.48}$$

As a consequence of the normality rule and Melan-Prager's evolution law (12.46), $\dot{\alpha}_{ij}^d$ is normal to the yield surface and (12.48) shows that $\dot{\alpha}_{ij}^d$ has the direction given by $s_{ij} - \alpha_{ij}^d$, cf. Fig. 12.14.

A comparison of (12.48) with (12.41) shows that the combined evolution function q_{ij} is given by

$$q_{ij} = \frac{3c}{2\sigma_{yo}}(s_{ij} - \alpha_{ij}^d)$$

Insertion of this expression as well as (12.38b) into (12.42) leads to

$$H = \frac{3}{2}c\,\frac{3(s_{ij} - \alpha_{ij}^d)(s_{ij} - \alpha_{ij}^d)}{2\sigma_{yo}^2}$$

which with the yield criterion (12.37) reduces to

$$H = \frac{3}{2}c \tag{12.49}$$

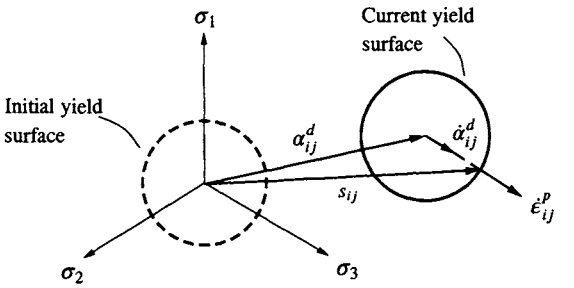

Figure 12.14: Illustration of Melan-Prager's evolution law in the deviatoric plane.

i.e. if c is constant, we have linear hardening. We emphasize that whereas (12.49) holds in general, the interpretation (12.45) only holds for uniaxial stress conditions.

Having established the fundamental elasto-plastic equations for kinematic hardening of a von Mises material, it is timely to discuss the prediction capabilities of this model.

The first issue of interest is the material parameter c appearing in the evolution law for the back-stress, cf. (12.46). The simplest choice is evidently to take c as a constant, but it is fully allowable to let c depend on some internal variable.

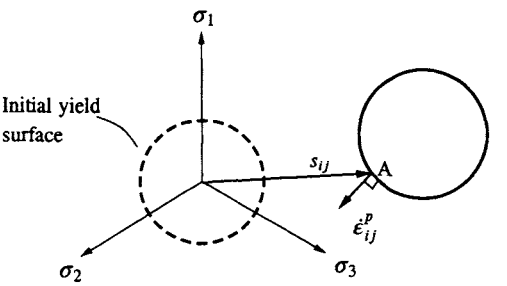

Figure 12.15: Deviatoric plane. The incremental plastic work $\dot{W}^p$ is negative when loading at point A, i.e. $\dot{W}^p = s_{ij}\dot{\epsilon}_{ij}^p < 0$.

We have previously, in the discussion of isotropic hardening of a von Mises material, used the plastic work W^p as an internal variable, cf. (9.73). Let us therefore investigate the consequences of assuming that

$$c = c(W^p) \quad \text{where} \quad \dot{W}^p = \sigma_{ij}\dot{\epsilon}_{ij}^p$$

In the present case, $\dot{\epsilon}_{ij}^p$ is purely deviatoric and the incremental plastic work may therefore also be written as

$$\dot{W}^p = s_{ij}\dot{\epsilon}_{ij}^p$$

It is of interest that whereas $\dot{W}^p$ is non-negative, i.e. $\dot{W}^p \geq 0$, for isotropic hardening of a von Mises material, cf. (9.76), this is not the case for kinematic hardening. Suppose that the current yield surface of the kinematic hardening von Mises material is located as shown in Fig. 12.15. It is evident that the scalar product $s_{ij}\dot{\varepsilon}^p_{ij}$ is negative, i.e. $\dot{W}^p < 0$, when plastic loading occurs at point A. For uniaxial stressing, the corresponding situation is shown in Fig. 12.16. According to (12.45) and (12.49), the slopes at point P and Q are identical. However, for uniaxial stressing we have $\dot{W}^p = \sigma_{ij}\dot{\varepsilon}^p_{ij} = \sigma\dot{\varepsilon}^p$; this means that $\dot{W}^p < 0$ when loading from point Q towards point R. Consequently, and as illustrated in Fig. 12.16, the slope will then increase when loading from point Q towards R. Clearly, this prediction is in contrast with experimental evidence and we can therefore reject the plastic work W^p as a suitable internal variable, when kinematic hardening is involved.

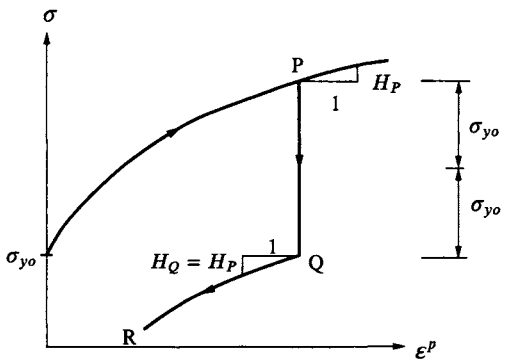

Figure 12.16: Consequence of letting $c = c(W^p)$, where $H = \frac{3}{2}c(W^p)$.

Let us next assume that the parameter c depends on the effective plastic strain, i.e.

$$c = c(\varepsilon^p_{eff}) \quad \text{where} \quad \dot{\varepsilon}^p_{eff} = (\frac{3}{2}\dot{\varepsilon}^p_{ij}\dot{\varepsilon}^p_{ij})^{1/2} = \dot{\lambda} \geq 0$$

Here, $\dot{\varepsilon}^p_{eff}$ is certainly non-negative, but even so the consequences of the assumption above are not promising.

To illustrate this, consider the uniaxial stressing shown in Fig. 12.17. The slopes at points P and Q are identical. Moreover, as $\dot{\varepsilon}^p_{eff} = |\dot{\varepsilon}^p|$ we find that the effective plastic strains ε^p_{eff} at points R and S are identical. Consequently and referring to Fig. 12.17, the slopes at points R and S are also identical and the response during reversed loading therefore becomes in inferior agreement with the real behavior of metals and steel.

The discussion above illustrates two important points. First, whereas it makes no difference for isotropic hardening of a von Mises material whether

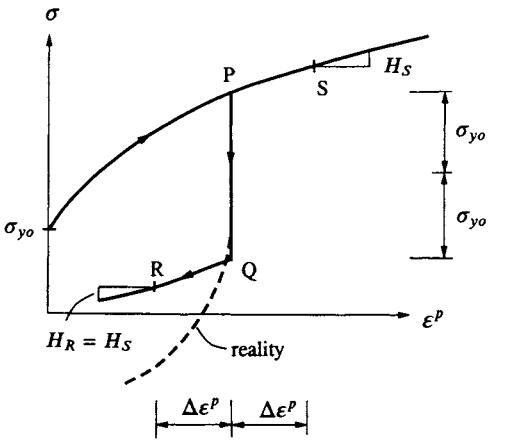

Figure 12.17: Consequence of letting $c = c(\varepsilon^p_{eff})$, where $H = \frac{3}{2}c(\varepsilon^p_{eff})$.

we adopt the plastic work or the effective plastic strain as internal variable, it makes a great difference when kinematic hardening is considered. Second, for kinematic hardening it is not trivial to obtain a realistic response for reversed loading, if the plastic modulus H is to vary with the loading.

In view of these latter difficulties, the classical approach is simply to assume that the parameter c is a constant, i.e. the plastic modulus $H = 3c/2$ is also constant and we then have linear hardening, i.e.

$$\boxed{H = \frac{3}{2}c = constant}$$

In the next chapter, we will return to more advanced kinematic models that allow for nonlinear hardening and provide a detailed discussion. For linear hardening, the response is illustrated in Fig. 12.18 and it appears that the Bauschinger effect is fairly well approximated even though the agreement with the real response is not overwhelming.

For stress cycling between the stresses σ_A and $-\sigma_A$, the linear kinematic model predicts the behavior shown in Fig. 12.19a). No cyclic hardening or softening effects can be predicted and the stabilized cyclic stress-strain curve is obtained already after one cycle. For strain cycling between ε_A and $-\varepsilon_A$, the prediction shown in Fig. 12.19b) is obtained. Since the stabilized cyclic stress-strain curve is obtained already after one cycle and since it is symmetric about the origin, there is no difference between stress cycling and strain cycling, cf. Figs. 12.19a) and 12.19b).

For cycling between unsymmetrical stress states, the result in Fig. 12.20a) is obtained; no ratcheting is predicted and the stabilized cyclic stress-strain curve is obtained already after one cycle. Similarly, Fig. 12.20b) shows unsymmetri-

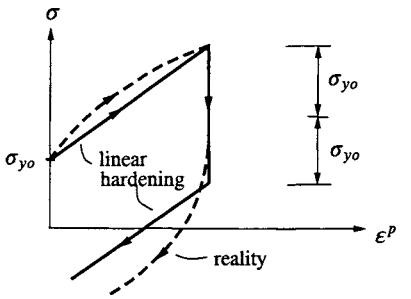

Figure 12.18: Prediction of kinematic hardening von Mises model with linear hardening, i.e. $H = \frac{3}{2}c$=constant.

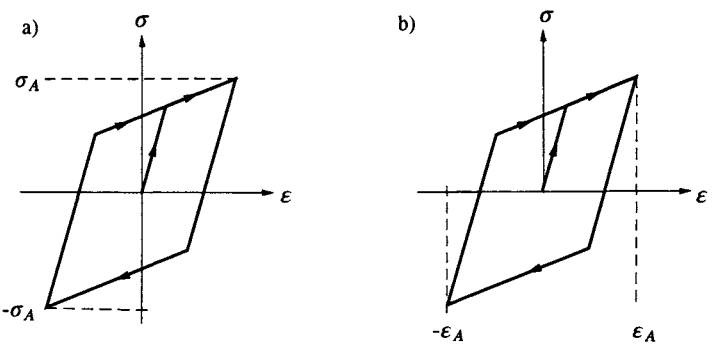

Figure 12.19: a) symmetrical stress cycling; b) symmetrical strain cycling.

cal strain cycling; no mean stress relaxation is predicted and since the stabilized cyclic stress-strain curve is obtained already after one cycle and since it is symmetric, there is no difference between stress cycling and strain cycling.

Even though linear kinematic hardening is not able to predict all important phenomena relating to cyclic behavior, it is evident that it is much more attractive than the isotropic hardening model when such loadings are of relevance.

Having illustrated that linear kinematic hardening of a von Mises material provides a first approximation when significant reversed loadings are of interest, we will now establish the tangential elasto-plastic stiffness matrix $\boldsymbol{D}^{ep}$ that is of importance in nonlinear finite element calculations.

Again, we assume elastic isotropy as given by (12.14), i.e. we obtain with (12.38a) and associated plasticity

$$\frac{\partial f}{\partial \sigma_{mn}} D_{mnkl} = \frac{3G}{\sigma_{yo}}(s_{kl} - \alpha^d_{kl}) \; ; \qquad D_{ijst} \frac{\partial f}{\partial \sigma_{st}} = \frac{3G}{\sigma_{yo}}(s_{ij} - \alpha^d_{ij})$$

From (10.24) and (12.37), it then follows that

$$A = H + 3G$$

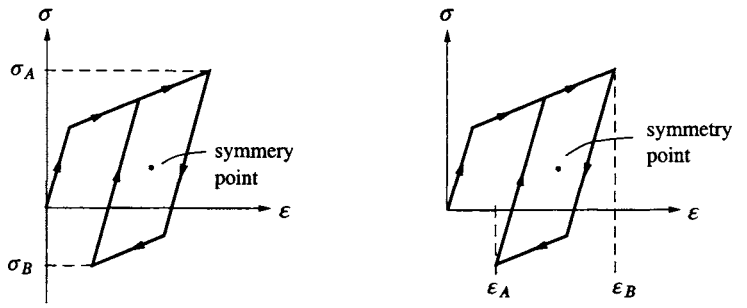

Figure 12.20: a) unsymmetrical stress cycling; b) unsymmetrical strain cycling.

Expressions (10.26) and (10.27) then lead to

$$\dot{\sigma}_{ij} = D^{ep}_{ijkl}\dot{\varepsilon}_{kl} \tag{12.50}$$

where

$$D^{ep}_{ijkl} = D_{ijkl} - \frac{9G^2}{A\sigma^2_{yo}}(s_{ij} - \alpha^d_{ij})(s_{kl} - \alpha^d_{kl})$$

If we express (12.50) in a matrix form similar to (4.37), we obtain

$$\dot{\boldsymbol{\sigma}} = \boldsymbol{D}^{ep}\dot{\boldsymbol{\varepsilon}} \tag{12.51}$$

where

$$\boldsymbol{D}^{ep} = \boldsymbol{D} - \boldsymbol{D}^{p}$$

and

$$\boldsymbol{D} = \frac{2G}{1-2\nu}\begin{bmatrix} 1-\nu & \nu & \nu & 0 & 0 & 0 \\ \nu & 1-\nu & \nu & 0 & 0 & 0 \\ \nu & \nu & 1-\nu & 0 & 0 & 0 \\ 0 & 0 & 0 & \frac{1}{2}(1-2\nu) & 0 & 0 \\ 0 & 0 & 0 & 0 & \frac{1}{2}(1-2\nu) & 0 \\ 0 & 0 & 0 & 0 & 0 & \frac{1}{2}(1-2\nu) \end{bmatrix} \tag{12.52}$$

$$\boldsymbol{D}^{p} = \frac{9G^2}{A\sigma^2_{yo}}\begin{bmatrix} \bar{s}^2_{11} & \bar{s}_{11}\bar{s}_{22} & \bar{s}_{11}\bar{s}_{33} & \bar{s}_{11}\bar{s}_{12} & \bar{s}_{11}\bar{s}_{13} & \bar{s}_{11}\bar{s}_{23} \\ \bar{s}_{22}\bar{s}_{11} & \bar{s}^2_{22} & \bar{s}_{22}\bar{s}_{33} & \bar{s}_{22}\bar{s}_{12} & \bar{s}_{22}\bar{s}_{13} & \bar{s}_{22}\bar{s}_{23} \\ \bar{s}_{33}\bar{s}_{11} & \bar{s}_{33}\bar{s}_{22} & \bar{s}^2_{33} & \bar{s}_{33}\bar{s}_{12} & \bar{s}_{33}\bar{s}_{13} & \bar{s}_{33}\bar{s}_{23} \\ \bar{s}_{12}\bar{s}_{11} & \bar{s}_{12}\bar{s}_{22} & \bar{s}_{12}\bar{s}_{33} & \bar{s}^2_{12} & \bar{s}_{12}\bar{s}_{13} & \bar{s}_{12}\bar{s}_{23} \\ \bar{s}_{13}\bar{s}_{11} & \bar{s}_{13}\bar{s}_{22} & \bar{s}_{13}\bar{s}_{33} & \bar{s}_{13}\bar{s}_{12} & \bar{s}^2_{13} & \bar{s}_{13}\bar{s}_{23} \\ \bar{s}_{23}\bar{s}_{11} & \bar{s}_{23}\bar{s}_{22} & \bar{s}_{23}\bar{s}_{33} & \bar{s}_{23}\bar{s}_{12} & \bar{s}_{23}\bar{s}_{13} & \bar{s}^2_{23} \end{bmatrix} \tag{12.53}$$

It is recalled that $\bar{s}_{ij} = s_{ij} - \alpha^d_{ij}$.

It may be of interest to observe that isotropic and kinematic von Mises hardening formally possess the same structure, cf. (12.19), (12.20) with (12.52) and (12.53). In fact, if we in (12.20) replace σ_y by σ_{y0} and s_{ij} by $\bar{s}_{ij}$ then (12.53) is obtained. This implies that the $\boldsymbol{D}^{ep}$-matrix for plane strain can be obtained directly from (12.21)-(12.24) whereas the $\boldsymbol{D}^{ep}$-matrix for plane stress can be established directly from (12.27) and (12.28)-(12.31).

12.4 Mixed von Mises hardening

We have discussed isotropic as well as kinematic hardening of a von Mises material and it seems tempting to investigate whether we can combine these models and thereby achieve additional freedom in our effort to model metals and steel in an accurate fashion.

In fact, we have previously, in (9.26) and (9.27), touched upon the concept of mixed hardening, which combines isotropic and kinematic hardening and which was introduced by Hodge (1957). Different mixed hardening formulations exist, but due to its usefulness we shall here adopt the formulation proposed by Goel and Malvern (1970), Krieg and Key (1976) and Axelsson and Samuelsson (1979). While this formulation holds for arbitrary yield functions, we will here restrict ourselves to mixed hardening of a von Mises material. The presentation will be given in fashion that is consistent with the previous exposition.

Within a von Mises concept and referring to (12.4) and (12.37), the yield criterion for mixed hardening reads

$$\boxed{f(\sigma_{ij}, K_\alpha) = [\frac{3}{2}(s_{kl} - \alpha^d_{kl})(s_{kl} - \alpha^d_{kl})]^{1/2} - \sigma_{yo} - K(\kappa) = 0} \tag{12.54}$$

where the deviatoric part of the back-stress α^d_{kl} and the parameter K are formally included in the hardening parameters K_α, i.e.

$$K_\alpha = \{\alpha^d_{ij}, K\} \tag{12.55}$$

We also note that K depends on the internal variable κ. It appears that if $K = 0$ then (12.54) reduces to purely kinematic hardening and if $\alpha^d_{ij} = 0$ then purely isotropic hardening is obtained. Let us define the quantity $\bar{\sigma}_y(\kappa)$ by

$$\boxed{\bar{\sigma}_y = \sigma_{yo} + K(\kappa)} \tag{12.56}$$

From (12.54) then follows that

$$\frac{\partial f}{\partial \sigma_{ij}} = \frac{3(s_{ij} - \alpha^d_{ij})}{2\bar{\sigma}_y}\,; \quad \frac{\partial f}{\partial \alpha^d_{ij}} = -\frac{3(s_{ij} - \alpha^d_{ij})}{2\bar{\sigma}_y}\,; \quad \frac{\partial f}{\partial K} = -1 \tag{12.57}$$

The associated flow rule then gives

$$\dot{\varepsilon}^p_{ij} = \dot{\lambda}\frac{3(s_{ij} - \alpha^d_{ij})}{2\bar{\sigma}_y} \tag{12.58}$$

which implies $\dot{\varepsilon}^p_{ii} = 0$, i.e. plastic incompressibility. This means that $\dot{\varepsilon}^p_{ij}$ is a purely deviatoric tensor. Define as usual the effective plastic strain rate by

$$\dot{\varepsilon}^p_{eff} = (\frac{2}{3}\dot{\varepsilon}^p_{ij}\dot{\varepsilon}^p_{ij})^{1/2}$$

With the flow rule (12.58) as well as the yield criterion (12.54), it then follows that

$$\dot{\varepsilon}^p_{eff} = \dot{\lambda} \tag{12.59}$$

In our mixed hardening formulation, we have two hardening parameters in terms of the parameter K and the deviatoric part α^d_{ij} of the back-stress, cf. (12.55). Referring to the general expression (10.15) for the evolution laws, we write

$$\begin{aligned} \dot{K} &= \dot{\lambda} q^{(1)} \quad \text{where} \quad q^{(1)} = \frac{\partial K}{\partial \kappa} k \\ \dot{\alpha}^d_{ij} &= \dot{\lambda} q^{(2)}_{ij} \quad \text{where} \quad q^{(2)}_{ij} = \frac{\partial \alpha^d_{ij}}{\partial \kappa_{kl}} k_{kl} \end{aligned} \tag{12.60}$$

where $q^{(1)}$ and $q^{(2)}_{ij}$ are the two combined evolution functions. The consistency relation is written in the standard format

$$\frac{\partial f}{\partial \sigma_{ij}} \dot{\sigma}_{ij} - H\dot{\lambda} = 0 \tag{12.61}$$

where the plastic modulus H, according to (10.17) and (12.60), is defined by

$$H = -\frac{\partial f}{\partial K} q^{(1)} - \frac{\partial f}{\partial \alpha^d_{ij}} q^{(2)}_{ij} \tag{12.62}$$

To obtain an interpretation of the plastic modulus H, we multiply (12.61) by $\dot{\lambda}$ and use the flow rule $\dot{\varepsilon}^p_{ij} = \dot{\lambda}\partial f / \partial \sigma_{ij}$ as well as (12.59) to obtain

$$\dot{\varepsilon}^p_{ij}\dot{\sigma}_{ij} - (\dot{\varepsilon}^p_{eff})^2 H = 0 \tag{12.63}$$

Considering uniaxial stressing, the term $\dot{\varepsilon}^p_{ij}\dot{\sigma}_{ij}$ reduces to $\dot{\varepsilon}^p\dot{\sigma}$ and $\dot{\varepsilon}^p_{eff}$ becomes equal to $|\dot{\varepsilon}^p|$. In this case, (12.63) reduces to

$$\boxed{\frac{d\sigma}{d\varepsilon^p} = H} \tag{12.64}$$

This interpretation is shown in Fig. 12.13.

The next step is to choose the specific form of the evolution functions $q^{(1)}$ and $q^{(2)}_{ij}$ present in (12.60). Inspired by the strain hardening assumption (12.13)

used for isotropic hardening and the Melan-Prager evolution law (12.46) for kinematic hardening, we choose

$$\boxed{\begin{aligned} \dot{K} &= \dot{\lambda} m \frac{dK}{d\kappa}\,; \\ \dot{\alpha}_{ij} &= (1-m) c \dot{\varepsilon}^p_{ij} \end{aligned}} \tag{12.65}$$

where the constant parameter m is called the *mixed hardening parameter* and it is chosen by us; moreover, we have $0 \leq m \leq 1$. It appears that if $m = 0$, then a purely kinematic hardening model emerges, whereas $m = 1$ implies a purely isotropic hardening model. For m between these two values, we have mixed hardening and this suggests the terminology of m being the mixed hardening parameter. From (12.65a) and (12.59) as well as $\dot{K} = \frac{dK}{d\kappa}\dot{\kappa}$, we conclude that

$$\kappa = m \varepsilon^p_{eff} \tag{12.66}$$

Since $\dot{\varepsilon}^p_{ij}$ is purely deviatoric, (12.65b) implies

$$\alpha^d_{ij} = \alpha_{ij} \tag{12.67}$$

Therefore, use of the flow rule (12.58) in (12.65b) gives

$$\dot{\alpha}^d_{ij} = \dot{\lambda}(1-m)\frac{3c}{2\bar{\sigma}_y}(s_{ij} - \alpha^d_{ij}) \tag{12.68}$$

and a comparison of (12.65a) and (12.68) with (12.60a) and (12.60b), respectively, results in

$$q^{(1)} = m\frac{dK}{d\kappa}\,; \qquad q^{(2)}_{ij} = (1-m)\frac{3c}{2\bar{\sigma}_y}(s_{ij} - \alpha^d_{ij}) \tag{12.69}$$

The plastic modulus H is defined by (12.62). Use of (12.57b) and (12.57c) as well as (12.69) then provide

$$H = \frac{dK(\kappa)}{d\kappa} m + \frac{3}{2} c(1-m)\frac{3(s_{ij} - \alpha^d_{ij})(s_{ij} - \alpha^d_{ij})}{2\bar{\sigma}^2_y}$$

which with the yield criterion reduces to

$$H = \frac{dK(\kappa)}{d\kappa} m + \frac{3}{2} c(1-m) \tag{12.70}$$

It is emphasized that whereas this expression holds in general, the interpretation (12.64) only holds for uniaxial stress conditions.

In order to determine the material properties $dK(\kappa)/d\kappa$ and c, we rewrite (12.70) according to

$$H = [\frac{dK(\kappa)}{d\kappa} - \frac{3}{2}c]m + \frac{3}{2}c \tag{12.71}$$

It is advantageous to construct the mixed hardening model such that irrespective of our choice for the parameter m, we obtain the same response for monotonic proportional loading. For all other load histories, however, the value of m influences the response and this is particularly true when reversed loadings are involved. Let us therefore investigate the consequences of monotonic proportional loading.

For monotonic proportional loading, we have

$$s_{ij} = p(t)s^*_{ij} \tag{12.72}$$

where $p(t)$ is an increasing function of time t and s^*_{ij} is an arbitrary fixed deviatoric stress tensor. Before any plasticity is involved, we have $\alpha^d_{ij} = 0$. Referring to the evolution law (12.68), this means that the first increment $\dot{\alpha}^d_{ij}$ (when $\alpha^d_{ij} = 0$) will be proportional to s_{ij} and thereby to s^*_{ij}. This allows us to conclude that for monotonic proportional loading, α^d_{ij} will be proportional to s^*_{ij}. With this result and (12.72), it is concluded that

$$s_{ij} - \alpha^d_{ij} = q(t)s^*_{ij} \tag{12.73}$$

where $q(t)$ is a function of time. From (12.61) and the flow rule, we have

$$\dot{\varepsilon}^p_{ij} = \frac{1}{H}\frac{\partial f}{\partial \sigma_{kl}}\dot{\sigma}_{kl}\frac{\partial f}{\partial \sigma_{ij}}$$

which with (12.57a) becomes

$$\dot{\varepsilon}^p_{ij} = \frac{1}{H}\frac{3(s_{kl} - \alpha^d_{kl})}{2\bar{\sigma}_y}\dot{\sigma}_{kl}\frac{3(s_{ij} - \alpha^d_{ij})}{2\bar{\sigma}_y}$$

Noting that $(s_{kl} - \alpha^d_{kl})\dot{\sigma}_{kl} = (s_{kl} - \alpha^d_{kl})\dot{s}_{kl}$, use of (12.73) yields

$$\dot{\varepsilon}^p_{ij} = \frac{1}{H}\frac{3qs^*_{kl}\dot{p}s^*_{kl}}{2\bar{\sigma}_y}\frac{3qs^*_{ij}}{2\bar{\sigma}_y} \tag{12.74}$$

Insertion of (12.73) into the yield criterion (12.54) leads to

$$|q|(\frac{3}{2}s^*_{kl}s^*_{kl})^{1/2} = \bar{\sigma}_y$$

Elimination of the term $s^*_{kl}s^*_{kl}$ in (12.74) then implies the result

$$\dot{\varepsilon}^p_{ij} = \frac{3}{2H}\dot{p}s^*_{ij}$$

and it is concluded that different plasticity models provide the same result for monotonic proportional loading, if the plastic modulus H is the same.

In view of (12.71), the requirement that the mixed hardening model should predict the same response for monotonic proportional loading irrespective of the value of the parameter m then leads to

$$\boxed{\frac{dK(\kappa)}{d\kappa} = \frac{3}{2}c\,; \qquad H = \frac{3}{2}c} \tag{12.75}$$

Linear hardening

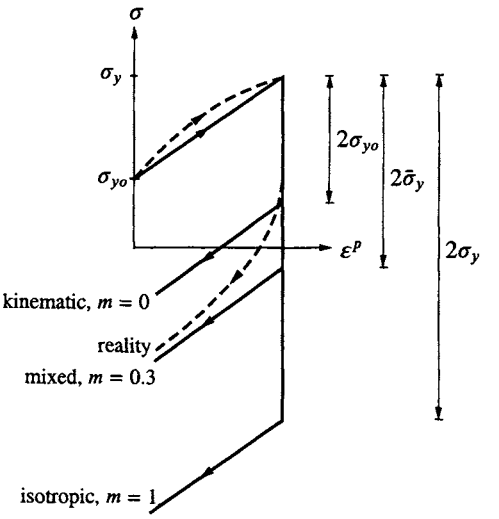

Figure 12.21: Prediction of mixed hardening von Mises model with linear hardening.

In order to proceed any further, the discussion in the previous section concerning purely kinematic hardening is recalled; it proved difficult to deal with a plastic modulus H that varies with the loading. In the following, we will therefore restrict ourselves to linear hardening, i.e.

$$\boxed{H = \frac{3}{2}c = constant} \tag{12.76}$$

Under these conditions, integration of (12.75a) yields $K = \frac{3}{2}c\kappa$, which with (12.66) and (12.56) leads to

$$\boxed{\bar{\sigma}_y = \sigma_{yo} + \frac{3}{2}cm\varepsilon^p_{eff}}$$

The predicted uniaxial response is illustrated in Fig. 12.21 from which also the interpretation of $\bar{\sigma}_y$ appears. It seems that by a proper choice of the mixed hardening parameter m, we can simulate a response during reversed loading that is in closer agreement with reality than the purely kinematic or purely isotropic model.

Let us in the following assume that the mixed hardening parameter is chosen as $m = 0.3$. For symmetric stress cycling between σ_A and $-\sigma_A$, the prediction is then shown in Fig. 12.22a). Cyclic hardening occurs and, eventually, after an infinite number of cycles, the response becomes purely elastic. For symmetric

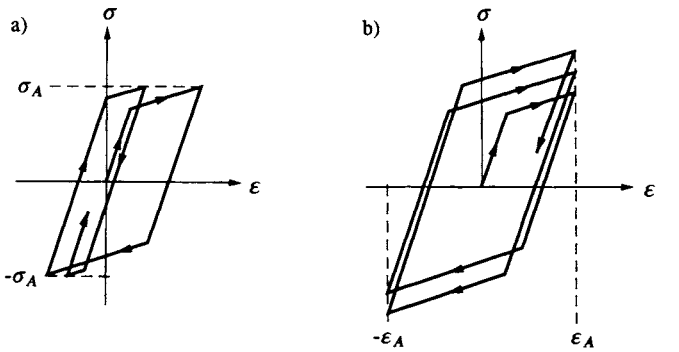

Figure 12.22: $m = 0.3$. a) symmetric stress cycling; b) symmetric strain cycling.

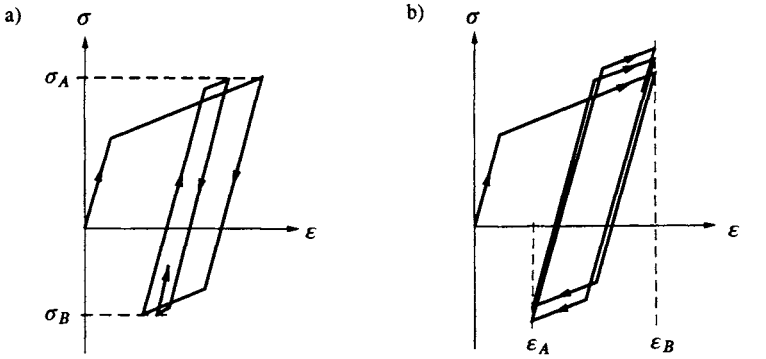

Figure 12.23: $m = 0.3$. a) unsymmetric stress cycling; b) unsymmetric strain cycling.

strain cycling between ε_A and $-\varepsilon_A$, the cyclic hardening response is shown in Fig. 12.22b) and, again, the stabilized cyclic behavior will be purely elastic. For unsymmetric stress cycling, the mixed hardening model predicts the response illustrated in Fig. 12.23a) and Fig. 12.23b) shows the situation of unsymmetric strain cycling.

In conclusion, when significant cyclic loadings are of relevance, mixed hardening offers advantages compared to purely isotropic or purely kinematic hardening, but even so, the mixed hardening model provides only a rather crude approximation to the real cyclic behavior.

Having discussed the prediction capabilities of mixed hardening, we turn to the establishment of the tangential elasto-plastic stiffness matrix $\boldsymbol{D}^{ep}$. Associated plasticity is adopted and elastic isotropy is again assumed, i.e. (12.14) together with (12.57a) yield

$$\frac{\partial f}{\partial \sigma_{mn}} D_{mnkl} = \frac{3G}{\bar{\sigma}_y}(s_{kl} - \alpha^d_{kl}) \; ; \qquad D_{ijst} \frac{\partial f}{\partial \sigma_{st}} = \frac{3G}{\bar{\sigma}_y}(s_{ij} - \alpha^d_{ij})$$

From (10.24) and (12.54), it follows that

$$A = H + 3G$$

Expressions (10.26) and (10.27) then lead to

$$\dot{\sigma}_{ij} = D^{ep}_{ijkl}\dot{\epsilon}_{kl} \tag{12.77}$$

where

$$D^{ep}_{ijkl} = D_{ijkl} - \frac{9G^2}{A\bar{\sigma}_y^2}(s_{ij} - \alpha^d_{ij})(s_{kl} - \alpha^d_{kl})$$

If we express (12.77) in a matrix form similar to (4.37), we obtain

$$\dot{\boldsymbol{\sigma}} = \boldsymbol{D}^{ep}\dot{\boldsymbol{\epsilon}}$$

where

$$\boldsymbol{D}^{ep} = \boldsymbol{D} - \boldsymbol{D}^{p}$$

and

$$\boldsymbol{D} = \frac{2G}{1-2\nu}\begin{bmatrix} 1-\nu & \nu & \nu & 0 & 0 & 0 \\ \nu & 1-\nu & \nu & 0 & 0 & 0 \\ \nu & \nu & 1-\nu & 0 & 0 & 0 \\ 0 & 0 & 0 & \frac{1}{2}(1-2\nu) & 0 & 0 \\ 0 & 0 & 0 & 0 & \frac{1}{2}(1-2\nu) & 0 \\ 0 & 0 & 0 & 0 & 0 & \frac{1}{2}(1-2\nu) \end{bmatrix} \tag{12.78}$$

$$\boldsymbol{D}^{p} = \frac{9G^2}{A\bar{\sigma}_y^2}\begin{bmatrix} \bar{s}_{11}^2 & \bar{s}_{11}\bar{s}_{22} & \bar{s}_{11}\bar{s}_{33} & \bar{s}_{11}\bar{s}_{12} & \bar{s}_{11}\bar{s}_{13} & \bar{s}_{11}\bar{s}_{23} \\ \bar{s}_{22}\bar{s}_{11} & \bar{s}_{22}^2 & \bar{s}_{22}\bar{s}_{33} & \bar{s}_{22}\bar{s}_{12} & \bar{s}_{22}\bar{s}_{13} & \bar{s}_{22}\bar{s}_{23} \\ \bar{s}_{33}\bar{s}_{11} & \bar{s}_{33}\bar{s}_{22} & \bar{s}_{33}^2 & \bar{s}_{33}\bar{s}_{12} & \bar{s}_{33}\bar{s}_{13} & \bar{s}_{33}\bar{s}_{23} \\ \bar{s}_{12}\bar{s}_{11} & \bar{s}_{12}\bar{s}_{22} & \bar{s}_{12}\bar{s}_{33} & \bar{s}_{12}^2 & \bar{s}_{12}\bar{s}_{13} & \bar{s}_{12}\bar{s}_{23} \\ \bar{s}_{13}\bar{s}_{11} & \bar{s}_{13}\bar{s}_{22} & \bar{s}_{13}\bar{s}_{33} & \bar{s}_{13}\bar{s}_{12} & \bar{s}_{13}^2 & \bar{s}_{13}\bar{s}_{23} \\ \bar{s}_{23}\bar{s}_{11} & \bar{s}_{23}\bar{s}_{22} & \bar{s}_{23}\bar{s}_{33} & \bar{s}_{23}\bar{s}_{12} & \bar{s}_{23}\bar{s}_{13} & \bar{s}_{23}^2 \end{bmatrix} \tag{12.79}$$

It is recalled that $\bar{s}_{ij} = s_{ij} - \alpha^d_{ij}$.

It is of interest that isotropic hardening and mixed hardening formally possess the same structure, cf. (12.19), (12.20) with (12.78) and (12.79). In fact, if we in (12.20) replace σ_y by $\bar{\sigma}_y$ and s_{ij} by $\bar{s}_{ij}$ then (12.79) is recovered. This implies that the $\boldsymbol{D}^{ep}$-matrix for plane strain can be obtained directly from (12.21)-(12.24) whereas the $\boldsymbol{D}^{ep}$-matrix for plane stress may be established directly from (12.27) and (12.28)-(12.31).

12.5 Melan-Prager's evolution law versus Ziegler's evolution law

The evolution law for the back-stress α_{ij} was previously given in the form suggested by Melan (1938) and Prager (1955), i.e.

$$\boxed{\dot{\alpha}_{ij} = c\,\dot{\varepsilon}^p_{ij} \qquad \textit{Melan-Prager's evolution law}} \tag{12.80}$$

cf. (12.46). With the flow rule, we obtain in general

$$\dot{\alpha}_{ij} = \dot{\lambda}\, c \frac{\partial g}{\partial \sigma_{ij}} \qquad \text{Melan-Prager} \tag{12.81}$$

which fits into the general format for evolution laws given by (10.15). For associated plasticity, this means that the direction of $\dot{\alpha}_{ij}$ is given by the normal to the yield surface at the current stress point as illustrated in Fig. 12.24a).

Another evolution law was proposed by Ziegler (1959) and it reads

$$\boxed{\dot{\alpha}_{ij} = \dot{\mu}(\sigma_{ij} - \alpha_{ij}) \qquad \textit{Ziegler's evolution law}} \tag{12.82}$$

where $\dot{\mu}$ is a non-negative quantity. This evolution law is illustrated in Fig. 12.24b). Since μ may be regarded as an internal variable, we can write the evolution law for μ in accordance with the general format given by (10.15), i.e

$$\dot{\mu} = \dot{\lambda} k \tag{12.83}$$

where k is a certain positive evolution function. Use of (12.83) in (12.82) implies

$$\dot{\alpha}_{ij} = \dot{\lambda} k(\sigma_{ij} - \alpha_{ij}) \qquad \text{Ziegler} \tag{12.84}$$

which fits into the general framework for evolution laws of hardening parameters given by (10.15).

In general, the two proposals (12.81) and (12.84) are different, but there are cases where they coincide. Assume that we have mixed hardening of a von Mises material. Since associated plasticity is assumed, Melan-Prager's evolution law (12.81) and (12.57a) give

$$\dot{\alpha}_{ij} = \dot{\lambda} \frac{3c}{2\bar{\sigma}_y}(s_{ij} - \alpha_{ij}) \; ; \qquad \alpha^d_{ij} = \alpha_{ij} \tag{12.85}$$

As indicated, this evolution law implies that α_{ij} is purely deviatoric. In the von Mises yield criterion only the deviatoric part α^d_{ij} of the back-stress enters. Therefore, if Ziegler's evolution law (12.84) is adopted, we obtain

$$\dot{\alpha}^d_{ij} = \dot{\lambda} k(s_{ij} - \alpha^d_{ij}) \tag{12.86}$$

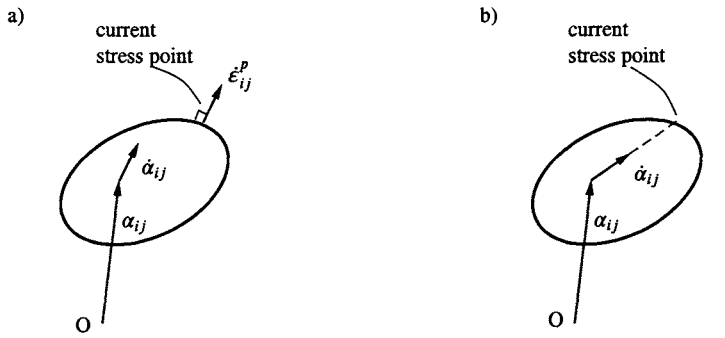

Figure 12.24: Illustration of evolution laws in the general stress space where O denotes the origin; a) Melan-Prager's rule for associated plasticity; b) Ziegler's rule.

It is noted that the hydrostatic part $\dot{\alpha}_{ii} = \dot{\lambda}k(\sigma_{ii} - \alpha_{ii})$ of the back-stress does not at all enter the mixed von Mises formulation. Moreover, a comparison of (12.85) and (12.86) reveals that the two evolution laws are identical and that we have

$$k = \frac{3c}{2\bar{\sigma}_y}$$

It is concluded that

For a mixed von Mises formulation, Melan-Prager's and Ziegler's evolution laws provide the same response	(12.87)

Despite this identity, the interpretation of the two evolution laws may be different. This may occur if the stress space considered is not the full nine-dimensional stress space defined by all the nine components of σ_{ij}, but rather some subspace. We shall first discuss these aspects in general terms and then provide a simple illustration.

For Melan-Prager's evolution law, two issues are here of importance. For associated plasticity, Melan-Prager's evolution law states that the direction of $\dot{\alpha}_{ij}$ is given by the normal to the yield surface at the current stress point, cf. Fig. 12.24a). This holds in the full nine-dimensional stress space, but not necessarily in some subspace. Moreover, for a mixed von Mises formulation the back-stress α^d_{ij} defines the center of the yield surface in the deviatoric plane. In some subspace, however, the quantity $\alpha^d_{ij} = \alpha_{ij}$ as determined by Melan-Prager's evolution law does not necessarily define the center.

For Ziegler's evolution law, however, the interpretation that α_{ij} defines the center of the yield surface is independent of whether we work in the full nine-dimensional stress space or some subspace. To see this, we observe that $\alpha_{ij} = 0$

holds initially. Assume now that in some subspace some component of σ_{ij} is always zero, say $\sigma_{13} = 0$. It follows from (12.82) that also the component α_{13} will always be zero. This implies that α_{ij} will always describe the center of the yield surface irrespective of what stress space we are considering. It follows from (12.82) that the interpretation that the direction of the center movement is given by the quantity $\sigma_{ij} - \alpha_{ij}$ holds irrespective of the stress space considered.

The observation that it is only in the full nine-dimensional stress space that Melan-Prager's evolution law predicts the movement of the center to occur in the direction given by the normal to the yield surface was first pointed out by Hodge (1957). A general analysis of this topic was given by Shield and Ziegler (1958) and further insight was provided by Clavout and Ziegler (1959) as well as by Ziegler (1959).

For a von Mises material, the two evolution laws predict the same response. For other materials, however, their predictions will differ, but at present there does not seem to exist conclusive experimental evidence that allows one to decide which of the two evolution laws is most accurate.

12.6 Orthotropic Hill plasticity

Anisotropic plasticity is of importance in many applications and orthotropy is of relevance for rolled profiles of steel and metals as well as paper, wood and ice. Formulations of orthotropic Hill plasticity have been presented, for instance, by Hill (1950), Hu (1956), Chen and Han (1988), de Borst and Feenstra (1990) and Schellekens and de Borst (1992). For ideal plasticity, the effect of anisotropy is more or less trivially considered since no hardening parameters or internal variables enter the formulation; however, for hardening or softening anisotropic plasticity the situation becomes more complex. Here, we shall present an approach for isotropic hardening of a Hill material. Hill's yield criterion was treated in Section 8.13 and the approach presented here provides a natural extension of the similar concept of an isotropic hardening von Mises material. It is recalled that Hill's criterion is of relevance for orthotropic materials.

Let us rewrite Hill's initial yield criterion given by (8.92) as

$$(\sigma_{yo}^2 \boldsymbol{s}^T \boldsymbol{P} \boldsymbol{s})^{1/2} - \sigma_{yo} = 0$$

where the constant material parameter σ_{yo} having the dimension of stress is defined by

$$\boxed{\sigma_{yo} = [\frac{3}{2(F+G+H)}]^{1/2}}$$

According to (8.96), the term $F + G + H$ is always positive. From (8.94), the

symmetric matrix $\boldsymbol{P}$ is defined by

$$\boldsymbol{P} = \begin{bmatrix} \tilde{\boldsymbol{P}} & \boldsymbol{0} \\ \boldsymbol{0} & \tilde{\boldsymbol{Q}} \end{bmatrix} \tag{12.88}$$

where

$$\tilde{\boldsymbol{P}} = \begin{bmatrix} F+G & -F & -G \\ -F & F+H & -H \\ -G & -H & G+H \end{bmatrix} \; ; \quad \tilde{\boldsymbol{Q}} = \begin{bmatrix} 2L & 0 & 0 \\ 0 & 2M & 0 \\ 0 & 0 & 2N \end{bmatrix} \tag{12.89}$$

From (8.98) and considering an isotropic material, it is recalled that if

$$3F = 3G = 3H = L = M = N = \frac{3}{2\sigma_{yo}^2} \quad \Rightarrow \quad \textit{von Mises} \tag{12.90}$$

then Hill's criterion degenerates to the criterion of von Mises where σ_{yo} now, as previously, denotes the initial yield stress.

To obtain isotropic hardening of a Hill material, we write

$$\boxed{f(\sigma_{ij}, K) = (\sigma_{yo}^2 \boldsymbol{s}^T \boldsymbol{P} \boldsymbol{s})^{1/2} - \sigma_y = 0 \; ; \quad \sigma_y(\kappa) = \sigma_{yo} + K(\kappa)} \tag{12.91}$$

where K is the hardening parameter and κ is an internal variable, not yet specified.

As already indicated, we have here abandoned the tensor notation since many anisotropic yield criteria are expressed in matrix notation. As shown in Section 8.13, structural tensors can be used to describe anisotropic yield criteria and then a tensorial formulation is obtained. However, for illustration purposes we will here adopt a matrix format. The elastic stiffness is then also expressed in matrix notation and Hooke's law reads

$$\dot{\boldsymbol{\sigma}} = \boldsymbol{D}(\dot{\boldsymbol{\varepsilon}} - \dot{\boldsymbol{\varepsilon}}^p) \tag{12.92}$$

where $\boldsymbol{D}$ for the orthotropic material in question is defined by (4.55).

Adopting associated plasticity, the flow rule states that $\dot{\varepsilon}_{ij}^p = \dot{\lambda} \partial f / \partial \sigma_{ij}$ and in matrix notation this is expressed as

$$\boxed{\dot{\boldsymbol{\varepsilon}}_p = \dot{\lambda} \frac{\partial f}{\partial \boldsymbol{\sigma}}} \tag{12.93}$$

The quantity $\dot{\boldsymbol{\varepsilon}}^p$ is defined in the same manner as $\boldsymbol{\varepsilon}$, i.e. the engineering shear strains enter this column matrix, cf. (4.35). To define the meaning of $\partial f / \partial \boldsymbol{\sigma}$ some caution must be shown. To illustrate this aspect, let us express the von Mises criterion as

$$f = [\frac{3}{2}(s_{11}^2 + s_{22}^2 + s_{33}^2 + s_{12}^2 + s_{21}^2 + s_{13}^2 + s_{31}^2 + s_{23}^2 + s_{32}^2)]^{1/2} - \sigma_y = 0$$

$$\Rightarrow \quad \text{for instance} \quad \frac{\partial f}{\partial \sigma_{12}} = \frac{3 s_{12}}{2 \sigma_y} \quad \text{i.e.} \quad \dot{\varepsilon}_{12}^p = \dot{\lambda} \frac{3 s_{12}}{2 \sigma_y}$$

in accordance with our previous results. However, if advantage is taken of the symmetry of the stress tensor, we may write

$$f = [\frac{3}{2}(s_{11}^2 + s_{22}^2 + s_{33}^2 + 2s_{12}^2 + 2s_{13}^2 + 2s_{23}^2)]^{1/2} - \sigma_y = 0$$

$$\Rightarrow \quad \text{for instance} \quad \frac{\partial f}{\partial \sigma_{12}} = \frac{3s_{12}}{\sigma_y} \quad \text{i.e.} \quad 2\dot{\varepsilon}_{12}^p = \dot{\lambda}\frac{\partial f}{\partial \sigma_{12}}$$

It is concluded, that if formulation (12.93) is adopted then we have the following interpretation:

$$\boxed{\frac{\partial f}{\partial \boldsymbol{\sigma}} = \begin{bmatrix} \frac{\partial f}{\partial \sigma_{11}} \\ \frac{\partial f}{\partial \sigma_{22}} \\ \frac{\partial f}{\partial \sigma_{33}} \\ \frac{\partial f}{\partial \sigma_{12}} \\ \frac{\partial f}{\partial \sigma_{13}} \\ \frac{\partial f}{\partial \sigma_{23}} \end{bmatrix} \quad \textit{if advantage is taken of the symmetry of the stress tensor when formulating the yield criterion}} \tag{12.94}$$

In the yield criterion (12.91) advantage was taken of the symmetry of the stress tensor, i.e. the interpretation (12.94) holds.

To determine $\partial f/\partial \boldsymbol{\sigma}$ from (12.91), we first note that the deviatoric stresses $\boldsymbol{s}$ may be written as

$$\boldsymbol{s} = (\begin{bmatrix} \boldsymbol{I} & \boldsymbol{0} \\ \boldsymbol{0} & \boldsymbol{I} \end{bmatrix} - \frac{1}{3}\begin{bmatrix} \boldsymbol{E} & \boldsymbol{0} \\ \boldsymbol{0} & \boldsymbol{0} \end{bmatrix})\boldsymbol{\sigma}$$

where $\boldsymbol{I}$, as usual, is the unit matrix whereas $\boldsymbol{E}$ is defined by

$$\boldsymbol{E} = \begin{bmatrix} 1 & 1 & 1 \\ 1 & 1 & 1 \\ 1 & 1 & 1 \end{bmatrix}$$

With the symmetric matrix $\boldsymbol{P}$ given by (12.88), we then obtain

$$\frac{\partial(\boldsymbol{s}^T\boldsymbol{P}\boldsymbol{s})}{\partial \boldsymbol{\sigma}} = 2(\frac{\partial \boldsymbol{s}}{\partial \boldsymbol{\sigma}})^T\boldsymbol{P}\boldsymbol{s} = 2(\begin{bmatrix} \boldsymbol{I} & \boldsymbol{0} \\ \boldsymbol{0} & \boldsymbol{I} \end{bmatrix} - \frac{1}{3}\begin{bmatrix} \boldsymbol{E} & \boldsymbol{0} \\ \boldsymbol{0} & \boldsymbol{0} \end{bmatrix})\begin{bmatrix} \tilde{\boldsymbol{P}} & \boldsymbol{0} \\ \boldsymbol{0} & \tilde{\boldsymbol{Q}} \end{bmatrix}\boldsymbol{s}$$

by using $\boldsymbol{I}$ and $\boldsymbol{E}$ as symmetric. Noting that $\boldsymbol{E}\tilde{\boldsymbol{P}} = \boldsymbol{0}$, we obtain

$$\frac{\partial(\boldsymbol{s}^T\boldsymbol{P}\boldsymbol{s})}{\partial \boldsymbol{\sigma}} = 2\boldsymbol{P}\boldsymbol{s}$$

The flow rule (12.93) in combination with (12.91) then leads to the following expression

$$\boxed{\dot{\boldsymbol{\varepsilon}}^p = \dot{\lambda}\frac{\sigma_{yo}^2}{\sigma_y}\boldsymbol{P}\boldsymbol{s}} \tag{12.95}$$

It is easily checked that plastic incompressibility, i.e. $\dot{\varepsilon}^p_{11} + \dot{\varepsilon}^p_{22} + \dot{\varepsilon}^p_{33} = 0$, holds - as expected.

Let us also observe that if we define the effective stress σ_{eff} by

$$\boxed{\sigma_{eff} = (\sigma^2_{yo} \boldsymbol{s}^T \boldsymbol{P} \boldsymbol{s})^{1/2}} \tag{12.96}$$

then the yield criterion (12.91) may be expressed as

$$\sigma_{eff} - \sigma_y = 0 \tag{12.97}$$

For an isotropic material, where (12.90) holds, we find that (12.96) reduces to $\sigma_{eff} = (\frac{3}{2} s_{ij} s_{ij})^{1/2}$, i.e. the familiar effective von Mises stress.

It turns out to be advantageous to invert the flow rule (12.95), i.e. express $\boldsymbol{s}$ in terms of $\dot{\boldsymbol{\varepsilon}}^p$. Referring to (12.88), this inversion is hampered by the fact that while the inverse of $\tilde{\boldsymbol{Q}}$ always exists, we have $\det \tilde{\boldsymbol{P}} = 0$, i.e. also $\det \boldsymbol{P} = 0$ holds. However, we note that if a matrix $\tilde{\boldsymbol{M}}$ exists such that

$$\tilde{\boldsymbol{M}} \tilde{\boldsymbol{P}} = \frac{1}{3} \begin{bmatrix} 2 & -1 & -1 \\ -1 & 2 & -1 \\ -1 & -1 & 2 \end{bmatrix} \tag{12.98}$$

then

$$\tilde{\boldsymbol{M}} \tilde{\boldsymbol{P}} \begin{bmatrix} s_{11} \\ s_{22} \\ s_{33} \end{bmatrix} = \begin{bmatrix} s_{11} \\ s_{22} \\ s_{33} \end{bmatrix} \tag{12.99}$$

This particular property hinges on the fact that $s_{11} + s_{22} + s_{33} = 0$. With $\tilde{\boldsymbol{P}}$ given by (12.89), inspection shows that the following symmetric matrix

$$\tilde{\boldsymbol{M}} = \frac{1}{3(FG + FH + GH)} \begin{bmatrix} F+H & F-G-H & -H \\ F-G-H & F+G & -G \\ -H & -G & 2F \end{bmatrix}$$

fulfills (12.98). Define the symmetric matrix $\boldsymbol{M}$ by

$$\boldsymbol{M} = \begin{bmatrix} \tilde{\boldsymbol{M}} & \boldsymbol{0} \\ \boldsymbol{0} & \tilde{\boldsymbol{Q}}^{-1} \end{bmatrix} \quad \text{where} \quad \tilde{\boldsymbol{Q}}^{-1} = \begin{bmatrix} \frac{1}{2L} & 0 & 0 \\ 0 & \frac{1}{2M} & 0 \\ 0 & 0 & \frac{1}{2N} \end{bmatrix}$$

Using (12.88) and (12.99), it then follows that

$$\boldsymbol{M} \boldsymbol{P} \boldsymbol{s} = \boldsymbol{s} \tag{12.100}$$

and (12.95) then provides

$$\boldsymbol{s} = \frac{\sigma_y}{\dot{\lambda} \sigma^2_{yo}} \boldsymbol{M} \dot{\boldsymbol{\varepsilon}}^p \tag{12.101}$$

With the results (12.100) and (12.101), it turns out to be possible to express the plastic multiplier $\dot{\lambda}$ in terms of the plastic stain rate components. For this purpose, multiply (12.95) by $\boldsymbol{s}^T$ and use (12.91) to obtain

$$\boldsymbol{s}^T \dot{\boldsymbol{\varepsilon}}^p = \dot{\lambda}\sigma_y \tag{12.102}$$

Insertion of (12.101) gives

$$\frac{\sigma_y}{\dot{\lambda}\sigma_{yo}^2}(\dot{\boldsymbol{\varepsilon}}^p)^T \boldsymbol{M}\dot{\boldsymbol{\varepsilon}}^p = \dot{\lambda}\sigma_y$$

where it was used that $\boldsymbol{M}$ is symmetric. This leads to the result sought for

$$\boxed{\dot{\lambda} = [\frac{(\dot{\boldsymbol{\varepsilon}}^p)^T \boldsymbol{M}\dot{\boldsymbol{\varepsilon}}^p}{\sigma_{yo}^2}]^{1/2}} \tag{12.103}$$

Note that apart from some constant material parameters, the plastic multiplier $\dot{\lambda}$ has now been expressed entirely in terms of the plastic strain rate components.

With these results, let us evaluate (12.103) for an isotropic material. In this case (12.90) holds, which implies

$$\boldsymbol{M} = \frac{4}{9}\sigma_{yo}^2 \begin{bmatrix} 1 & -\frac{1}{2} & -\frac{1}{2} & 0 & 0 & 0 \\ -\frac{1}{2} & 1 & -\frac{1}{2} & 0 & 0 & 0 \\ -\frac{1}{2} & -\frac{1}{2} & 1 & 0 & 0 & 0 \\ 0 & 0 & 0 & \frac{3}{4} & 0 & 0 \\ 0 & 0 & 0 & 0 & \frac{3}{4} & 0 \\ 0 & 0 & 0 & 0 & 0 & \frac{3}{4} \end{bmatrix}$$

Insertion into (12.103) and using $\dot{\varepsilon}_{11}^p + \dot{\varepsilon}_{22}^p + \dot{\varepsilon}_{33}^p = 0$ lead to

$$\dot{\lambda} = \{\frac{2}{3}[(\dot{\varepsilon}_{11}^p)^2 + (\dot{\varepsilon}_{22}^p)^2 + (\dot{\varepsilon}_{33}^p)^2 + \frac{1}{2}(2\dot{\varepsilon}_{12}^p)^2 + \frac{1}{2}(2\dot{\varepsilon}_{13}^p)^2 + \frac{1}{2}(2\dot{\varepsilon}_{23}^p)^2]\}^{1/2}$$

i.e. $\dot{\lambda} = (2\dot{\varepsilon}_{ij}^p \dot{\varepsilon}_{ij}^p/3)^{1/2}$. It appears that $\dot{\lambda}$ for an isotropic material reduces to the previously defined effective plastic strain rate $\dot{\varepsilon}_{eff}^p$, cf. (12.9).

For orthotropic materials, it therefore seems natural also to define the effective plastic strain rate by

$$\boxed{\dot{\varepsilon}_{eff}^p = \dot{\lambda}} \tag{12.104}$$

where $\dot{\lambda}$ is given by (12.103). We may note that this definition leads to the following expression for the rate of plastic work

$$\dot{W}^p = \boldsymbol{\sigma}^T \dot{\boldsymbol{\varepsilon}}^p = \boldsymbol{s}^T \dot{\boldsymbol{\varepsilon}}^p = \dot{\lambda}\sigma_y$$

where (12.102) was used. Taking advantage of (12.104) and the yield criterion (12.97), we find the following simple expression

$$\boxed{\dot{W}^p = \sigma_y \dot{\varepsilon}^p_{eff} = \sigma_{eff} \dot{\varepsilon}^p_{eff}} \tag{12.105}$$

Expression (12.105) is in complete analogy with (9.76) applicable for a von Mises material.

In matrix notation, the consistency relation (10.16) reads

$$(\frac{\partial f}{\partial \boldsymbol{\sigma}})^T \dot{\boldsymbol{\sigma}} - H\dot{\lambda} = 0 \tag{12.106}$$

where the plastic modulus H according to (10.17) is defined by

$$H = -\frac{\partial f}{\partial K}\frac{\partial K}{\partial \kappa}k \tag{12.107}$$

and

$$\dot{\kappa} = \dot{\lambda}k \tag{12.108}$$

cf. (10.13). Just as for von Mises plasticity, we shall assume *strain hardening*, i.e.

$$\dot{\kappa} = \dot{\varepsilon}^p_{eff} \tag{12.109}$$

Since $\dot{\varepsilon}_{eff} = \dot{\lambda}$ we conclude from (12.108) that $k = 1$ and in view of (12.91), we have $\partial f/\partial K = -1$, i.e. (12.107) reduces to

$$H = \frac{\partial K}{\partial \kappa} \tag{12.110}$$

From (12.91) and (12.109) we have

$$\frac{\partial K}{\partial \kappa} = \frac{d\sigma_y(\varepsilon^p_{eff})}{d\varepsilon^p_{eff}}$$

i.e. (12.110) gives

$$\boxed{H = \frac{d\sigma_y(\varepsilon^p_{eff})}{d\varepsilon^p_{eff}}} \tag{12.111}$$

in complete analogy with von Mises plasticity, cf. (12.12).

Let us next illustrate how it is possible to calibrate the model by means of a uniaxial tension experiment. For uniaxial tension, the yield criterion (12.91) reduces to

$$\sigma_y = \sigma_{yo}\sigma_{11}\sqrt{F+G} \tag{12.112}$$

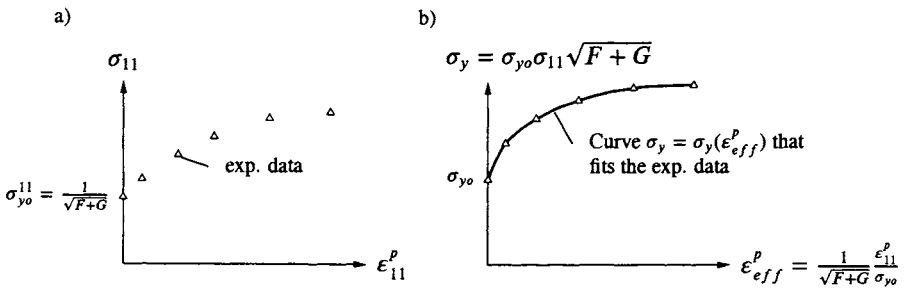

Figure 12.25: Uniaxial tension; a) original experimental data in a $\sigma_{11}, \varepsilon_{11}^p$-diagram, b) data transformed to a $\sigma_y, \varepsilon_{eff}^p$-diagram.

where initial yielding is obtained for $\sigma_y = \sigma_{yo}$, cf. (12.91), i.e. $\sigma_{11} = 1/\sqrt{F+G}$. From the flow rule (12.95), we find $2\dot{\varepsilon}_{12}^p = 2\dot{\varepsilon}_{13}^p = 2\dot{\varepsilon}_{23}^p = 0$ as well as

$$\begin{bmatrix} \dot{\varepsilon}_{11}^p \\ \dot{\varepsilon}_{22}^p \\ \dot{\varepsilon}_{33}^p \end{bmatrix} = \dot{\lambda}\frac{\sigma_{yo}^2}{\sigma_y}\sigma_{11}\begin{bmatrix} F+G \\ -F \\ -G \end{bmatrix}$$

Use of (12.112) then gives

$$\dot{\varepsilon}_{11}^p = \dot{\lambda}\frac{\sigma_{yo}^2}{\sigma_y}\sigma_{11}(F+G) = \dot{\lambda}\sigma_{yo}\sqrt{F+G}$$

and as $\dot{\lambda} = \dot{\varepsilon}_{eff}^p$, we obtain

$$\dot{\varepsilon}_{eff}^p = \frac{1}{\sqrt{F+G}}\frac{\dot{\varepsilon}_{11}^p}{\sigma_{yo}} \tag{12.113}$$

From (12.105), (12.112) and (12.113) we may note that $\dot{W}^p = \sigma_y\dot{\varepsilon}_{eff}^p = \sigma_{11}\dot{\varepsilon}_{11}^p$. However, returning to the calibration process we plot the experimental results in a stress (σ_{11})– plastic strain (ε_{11}^p) diagram, as shown in Fig. 12.25a). These data are converted into the data points shown in Fig. 12.25b) and approximated by the curve $\sigma_y = \sigma_y(\varepsilon_{eff}^p)$, which is now a known expression and (12.111) is then used to determine the plastic modulus H.

Let us finally determine the elasto-plastic stiffness matrix. From Hooke's law (12.92), the flow rule (12.93) and the consistency relation (12.106) we obtain in complete analogy with the procedure described in Chapter 10 that

$$\dot{\boldsymbol{\sigma}} = \boldsymbol{D}^{ep}\dot{\boldsymbol{\varepsilon}}$$

where the elasto-plastic stiffness matrix is given by

$$\boldsymbol{D}^{ep} = \boldsymbol{D} - \frac{1}{A}\boldsymbol{D}\frac{\partial f}{\partial \boldsymbol{\sigma}}\left(\frac{\partial f}{\partial \boldsymbol{\sigma}}\right)^T\boldsymbol{D}$$

and the positive parameter A is defined by

$$A = H + (\frac{\partial f}{\partial \sigma})^T \boldsymbol{D} \frac{\partial f}{\partial \sigma}$$

In the present case of orthotropy, the elastic stiffness matrix $\boldsymbol{D}$ is given by (4.55). Moreover, from (12.93) and (12.95) we have

$$\frac{\partial f}{\partial \sigma} = \frac{\sigma_{yo}^2}{\sigma_y} \boldsymbol{P}\boldsymbol{s}$$

This leads to

$$A = H + (\frac{\sigma_{yo}^2}{\sigma_y})^2 \boldsymbol{s}^T \boldsymbol{P}\boldsymbol{D}\boldsymbol{P}\boldsymbol{s}$$

and

$$\boldsymbol{D}^{ep} = \boldsymbol{D} - \boldsymbol{D}^p$$

where

$$\boldsymbol{D}^p = \frac{1}{A}(\frac{\sigma_{yo}^2}{\sigma_y})^2 \boldsymbol{D}\boldsymbol{P}\boldsymbol{s}\boldsymbol{s}^T\boldsymbol{P}\boldsymbol{D}$$

As a concluding remark to the above derivations, let us remember that the coordinate system was selected such that it coincides with the orthotropic material directions. If this is not the case *a priori*, the transformation rules for matrices, cf. Section 4.5, must first be used to achieve this situation.

12.7 Drucker-Prager plasticity. Frictional materials

So far, we have discussed common plasticity models for steel and metals, which all deal with various von Mises formulations; these materials are characterized by plastic incompressibility. To obtain an idea of how to model frictional materials like concrete, soil and rocks, we will consider *Drucker-Prager plasticity*. This formulation gives rise to plastic volume changes that are most characteristic for frictional materials; however, it will turn out that accurate predictions of these important plastic volume changes require much more than just a simple Drucker-Prager formulation. In this section we will provide an indication of the fundamental problems.

Referring to (8.33), isotropic hardening of a Drucker-Prager material is given by

$$f = 0; \quad \text{where} \quad f = \sigma_{eff} + \alpha I_1 - \beta - K \tag{12.114}$$

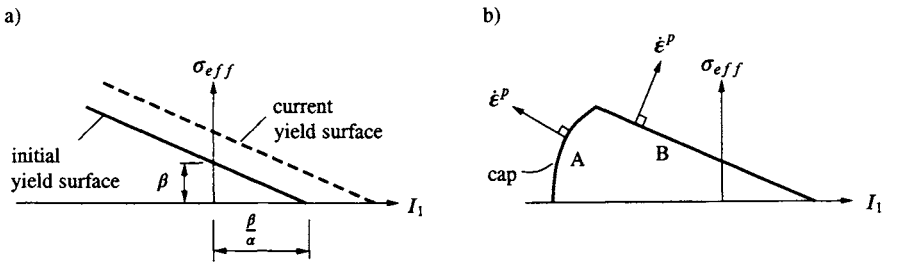

Figure 12.26: a) Isotropic hardening of Drucker-Prager material, b) Drucker-Prager yield surface supplemented by a cap.

where α and β are positive constants and the hardening parameter depends on an internal variable, i.e. $K = K(\kappa)$, cf. Fig. 12.26a). Adopting associated plasticity, we obtain

$$\dot{\varepsilon}_{ij}^p = \dot{\lambda}\frac{\partial f}{\partial \sigma_{ij}} = \dot{\lambda}\left(\frac{3s_{ij}}{2\sigma_{eff}} + \alpha\delta_{ij}\right); \qquad \dot{\kappa} = -\dot{\lambda}\frac{\partial f}{\partial K} = \dot{\lambda} \tag{12.115}$$

It follows that

$$\dot{\varepsilon}_{ii}^p = 3\dot{\lambda}\alpha \tag{12.116}$$

and a plastic volume increase is present. This volumetric plastic strain is only a very crude approximation of what happens in reality. Consider, for instance, purely hydrostatic compression of concrete where experimental data are shown in Fig. 4.9. It is evident that the nonlinear relation between hydrostatic stress and volumetric strain shown there can never be simulated by Drucker-Prager plasticity. According to Fig. 12.26a), purely hydrostatic compression of a Drucker-Prager material results in a linear elastic response.

To remedy this unfortunate situation, DiMaggio and Sandler (1971) added a yield surface, a so-called *cap*, to the Drucker-Prager yield surface. As shown in Fig. 12.26b), this cap closes the stress space so that purely hydrostatic compression will introduce plasticity; often, this cap is taken as part of an ellipse. According to the discussion relating to Fig. 12.7 and (12.3), it is concluded that at point A in Fig. 12.26b), we have $\dot{\varepsilon}_{ii}^p < 0$ whereas at point B, $\dot{\varepsilon}_{ii}^p > 0$ holds.

If the cap is taken to be part of an ellipse then

$$f_{cap} = 0; \quad \text{where} \quad f_{cap} = (I_1 - c)^2 + \sigma_{eff}^2 - q \tag{12.117}$$

where $(c, 0)$ denotes the center of the ellipse in the I_1, σ_{eff}-coordinate system. The parameters c and q in (12.117 both depend on hardening parameters.

Despite the progress achieved by introducing a cap, in practice it turns out that accurate modeling of the important plastic volume changes occurring in

frictional materials cannot be captured by the model described. With associated plasticity, the plastic volume change is controlled by the form of the yield surface in the meridian plane, cf. Fig. 12.26b). This is an all too restricted format and nonassociated plasticity is therefore adopted. We have

> *For frictional materials, the general experience is:*
> *Associated plasticity is used for the deviatoric response.*
> *Nonassociated plasticity is used for the volumetric response* (12.118)

In Section 22.3 we will return to Drucker-Prager plasticity and find that in order to fulfill the second law of thermodynamics, both associated and nonassociated Drucker-Prager plasticity are subject to certain nontrivial restrictions.

In addition to these complications, we have previously observed in (8.25) that it is not sufficient to consider the stress invariants I_1 and J_2 as was done by the model in Fig. 12.26b); for frictional materials, the third stress invariant in terms of the quantity $\cos 3\theta$ is of major influence. Thus, frictional materials require a nonassociated formulation and the yield criterion must consider the effect of all three stress invariants.

A model for soil that contains these ingredients was proposed by Lade (1977). In Fig. 12.26b) what corresponds to the cap and the Drucker-Prager yield surface was combined by Lade (1977) into one yield surface. This idea was further developed and refined by Lade and Kim (1995) and a somewhat similar concept was suggested by Krenk (2000) and Ahadi and Krenk (2000). In fact, a number of soil models exists in the literature and the same applies to concrete where we take the opportunity to refer to Schreyer and Babcock (1985), Faruque and Chang (1990), Lubarda *et al.* (1994) together with the textbooks of Chen and Han (1988) and Chen (1994) for additional information.